Strategical planning of Blue-Green Infrastructure: a multi-scale landscape connectivity approach for biodiversity enhancement

Master Thesis

Francesc Molné Correig

École Polytechnique Fédérale de Lausanne (EPFL)

Plant Ecology Research Laboratory (PERL)

Dr. Christoph Bachofen

Swiss Federal Institute of Aquatic Science and Technology (EAWAG)

Department of Urban Water Management (SWW)

Dr. Peter M. Bach
Dr. Giulia Donati

Swiss Federal Institute for Forest, Snow and Landscape Research (WSL)

Land-Use Systems Research Group

Dr. Janine Bolliger

MSc Environmental Sciences and Engineering

April, 2022

Abstract

Urban sprawl is a major driver of habitat degradation and fragmentation, resulting in declines in biodiversity worldwide. Blue-green infrastructures (BGI) can be highly relevant for maintaining a backbone of connected habitats. However, they are generally planned for other functions. This is partly because urban models (i.e. UrbanBEATS), which rely on spatial networks of dataset blocks representing local neighbourhoods, lack ecological information; while landscape connectivity models, which are generally based on high resolution raster grids and computationally intense operations, do not adequately represent urban space.

As part of the Swiss Blue-Green Biodiversity Research Initiative, this study addresses the need to integrate the merits of landscape ecology with detailed urban planning, including a case study in the cantons of Zürich and Aargau and focusing on four ecologically distinct amphibian species. First, we assess the performance of different spatial representations and resolutions to model circuit theory-based functional connectivity and simplify the model setup. Then, we apply spatial network analysis methods to identify priority urban areas for BGI implementation. Finally, we select top priority areas where we model high resolution structural connectivity to assess the local scale permeability of the areas.

Our findings will guide the development of a biodiversity module in UrbanBEATS and aim to provide practitioners with an optimized methodological framework for strategical BGI implementation in urban settings.

Keywords: biodiversity, blue-green infrastructure, functional connectivity, structural connectivity, network analysis, strategical planning, multi-scale.

Résumé

L'étalement urbain est l'un des principaux facteurs de dégradation et de fragmentation des habitats, ce qui entraîne un déclin de la biodiversité dans le monde entier. Les infrastructures bleu-vert (IBV) peuvent être très utiles pour maintenir une colonne vertébrale d'habitats connectés. Cependant, elles sont généralement planifiées pour d'autres fonctions. Cela s'explique en partie par le fait que les modèles urbains (par exemple UrbanBEATS), qui reposent sur des réseaux spatiaux de blocs de données représentant des quartiers locaux, manquent d'informations écologiques, tandis que les modèles de connectivité des paysages, qui sont généralement basés sur des grilles matricielles à haute résolution et des opérations intensives en calcul, ne représentent pas correctement l'espace urbain.

Dans le cadre de l'initiative suisse de recherche sur la biodiversité Blue-Green, cette étude répond au besoin d'intégrer les mérites de l'écologie du paysage à la planification urbaine détaillée, en incluant une étude de cas dans les cantons de Zürich et d'Argovie et en se concentrant sur quatre espèces d'amphibiens écologiquement distinctes. Tout d'abord, nous évaluons la performance de différentes représentations et résolutions spatiales pour modéliser la connectivité fonctionnelle basée sur la théorie des circuits et simplifier la configuration du modèle. Ensuite, nous appliquons des méthodes d'analyse de réseau spatial pour identifier les zones urbaines prioritaires pour la mise en œuvre de la BGI. Enfin, nous sélectionnons les zones prioritaires où nous modélisons la connectivité structurelle à haute résolution pour évaluer la perméabilité à l'échelle locale des zones.

Nos résultats guideront le développement d'un module de biodiversité dans UrbanBEATS et visent à fournir aux praticiens un cadre méthodologique optimisé pour la mise en œuvre stratégique de la BGI en milieu urbain.

Acknowledgements

I would like to thank all the people who have supported me during this Thesis on the past 6 months. The experience of having worked at EAWAG has been a great opportunity and I feel grateful for having had so competent and enriching people around. In particular, thanks to my supervisors Dr. Peter Bach, Dr. Giulia Donati, and Dr. Christoph Bachofen for offering me this interesting topic, the time spent for my concerns, the many interesting discussions we had and for all what I have learned from them. It has also been a privilege to collaborate with Dr. Janine Bolliger and get to know the WSL. Lastly, a special gratitude is dedicated to all the new friends from C10, as well as my family and friends who have supported and encouraged me in numerous ways during my studies.

Contents

1 Introduction

1.1 Background

Anthropogenic pressure, and more particularly urban sprawl and agricultural intensification, are causing the degradation and fragmentation of habitats, threatening species distribution and resulting in declines of biodiversity and ecosystem services worldwide (Horváth et al. (2019)). Ecological connectivity preservation and restoration of degraded areas have therefore become a top priority concern for conservation (Beier et al. (2006)).

In degraded human-dominated landscapes (HDLs) key biological processes such as breeding, dispersal, migration and resource utilization are interrupted (Fletcher Jr et al. (2018)), leading to gene flow reductions and significant impacts on genetic diversity and adaptive processes (Cayuela et al. (2018)).

According to the 17th edition of the Global Risks Report (World Economic Forum (2022)), biodiversity loss ranks as the third most severe risk on a global scale over the next 10 years, with four others in the top-ten list being likewise environment-related. As a result of species extinction and/or reduction, *"biodiversity loss implies a permanent destruction of natural capital with irreversible consequences for the environment, humankind, and economic activity"*, and should be strategically addressed.

Ecological infrastructures such as protected areas are useful mitigation measures. Yet, the long term effectiveness of these zones can be compromised by unsustainable urban development and agricultural intensification. Indeed, the contradiction between human developments and ecological conservation is increasingly prominent (Wu (2014)).

To address this challenge, Blue-Green Infrastructures (BGI) are emerging mitigation solutions, by which urban planners can coordinate the relationship between urban growth and ecosystem services (Pascual-Hortal and Saura (2006)).

In the following sections, a series of background concepts are reviewed, including the state-of-the-art of common Blue-Green Infrastructure technologies, landscape ecology methods and decision-support tools for urban planning.

1.1.1 Blue-Green Infrastructure (BGI)

The concept of Blue-Green Infrastructure has existed for decades, known although under several names, including Water Sensitive Urban Design (WSUD), Sustainable Urban Drainage Systems (SUDS), or Low Impact Development (LID) (Matsler et al. (2021)). The European Commission (2013) defines Green Infrastructure as *"a strategically planned network of natural and semi-natural areas with other environmental features designed and managed to deliver a wide range of ecosystem services such as water purification, air quality, space for recreation and climate mitigation and adaptation. This network of green (land) and blue (water) spaces can improve environmental conditions and therefore citizens' health and quality of life. It also supports a green economy, creates job opportunities and enhances biodiversity".* The EU Strategy on Green Infrastructure, and the EU 2030 Biodiversity Strategy (European Commission (2020)), promote investments in green infrastructure to restore ecosystems and ensure their functional connectivity.

One of the key attractions of green infrastructure is its multi-functionality. Contrary to single-purpose, traditional grey infrastructure, green and blue spaces can provide a wide variety of beneficial functions, simultaneously and at a fraction of the cost (European Commission (2019)). In terms of biodiversity, high-quality green spaces can increase the number and variety of species, functioning as urban biodiversity hotspots or stepping stones for otherwise fragmented ecosystems (Davis et al. (2015)). However, many BGI technologies in cities have been designed with stormwater management as the main objective, with other multiple functions (e.g. biodiversity support or urban heat reduction) treated as secondary benefits rather than baseline requirements. In the *Design Guidelines for Active, Beautiful, and Clean Waters*, PUB Singapore (2014) describe some typical vegetated treatment elements for the purification, detention, retention, conveyance, and infiltration of stormwater; including: vegetated swales, bioretention swales, bioretention basins (rain gardens), sedimentation basins, constructed wetlands, and cleansing biotopes (see Figure 1.1).

In fact, while those in charge of urban water management are somehow aware of these opportunities, there are still a number of hurdles to overcome, as well as some hesitation from urban planners and decision makers to take advantage of the full potential of these green systems (Bacchin et al. (2016)). To promote sustainable development, Monteiro et al. (2020) selected eight planning principles for BGI: connectivity, multifunctionality, applicability, integration, diversity, multiscale, governance, and continuity. Considering the magnitude of the risk of biodiversity loss, and in alignment with the EU biodiversity strategy, it is specially important to further develop, preserve and enhance healthy green infrastructure by implementing corridor structures and dense enough stepping-stone configurations, enabling ecosystems to deliver their many services to people and the environment (van der Sluis and Jongman (2021)). The greater the scale, coherence and connectivity of the green infrastructure network, the greater its positive impacts (European Commission (2013)).

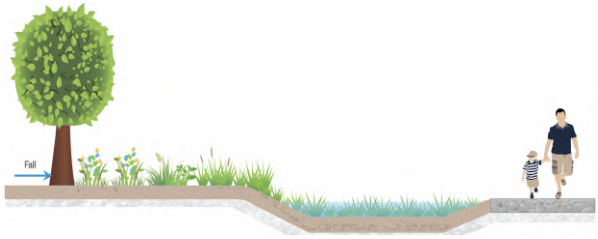

(a) Vegetated swales

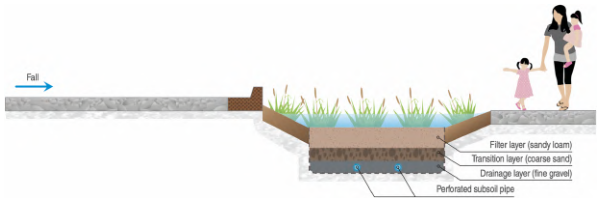

(b) Bioretention swales

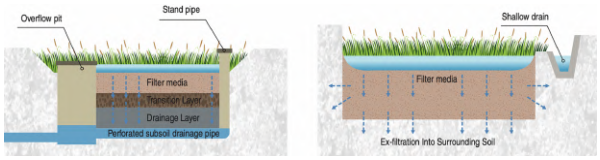

(c) Bioretention basins (rain gardens)

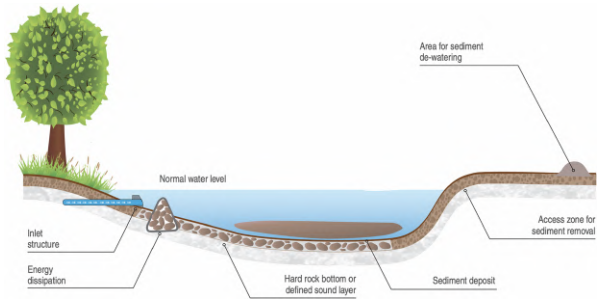

(d) Sedimentation basins

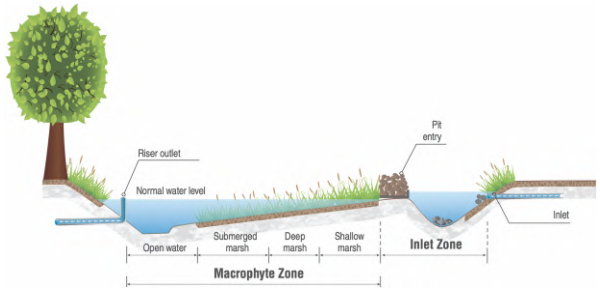

(e) Constructed wetlands

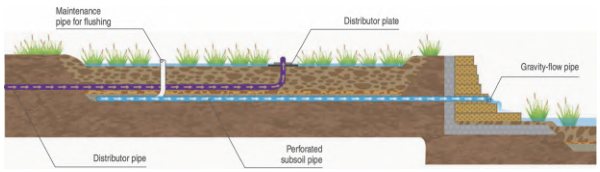

(f) Cleansing biotopes

Figure 1.1. BGI technologies for urban water management.
Source: PUB Singapore (2014).

1.1.2 Landscape connectivity

Taylor et al. (1993) defined landscape connectivity as *"the degree to which the landscape facilitates or impedes movement among resource patches"*. Landscape ecology studies connectivity and its vital role to maintain biodiversity and species interactions while promoting numerous ecosystem services. Within urban areas, functional corridors enable the migration and dispersal of certain species, serving as transit and recreation corridors for humans at the same time (Monteiro et al. (2020)). The potential of urban areas to support biodiversity and to connect their citizens to nature is, indeed, increasingly recognized (LaPoint et al. (2015)).

1.1.3 Landscape spatial representations

In connectivity modeling, landscape is analyzed from its underlying structure, that is the position, size, and architecture of its different features (Diniz et al. (2020)). Research has been centered in two spatial representations of the landscape (Figure 1.2), with their pros and cons described below:

Patch-based representations (Figure 1.2(a)) display spatial relationships among habitat sites through a network topology (Urban and Keitt (2001)). In these models, patches of habitat, defined for a focal species, are distinguished from the landscape matrix and constitute the nodes of the network. The connections between nodes are called edges, and represent the potential for movement or dispersal of a focal species (Galpern et al. (2011), Urban et al. (2009)). Within this spatial structure, an organism will potentially move through any connection inside a component, i.e. a group of connected nodes. Models based on this kind of representations can result in biologically plausible, computationally efficient, but suboptimal solutions (Cushman et al. (2013)).

Grid-based representations (Figure 1.2(b)) represent the landscape as a series of tessellated shapes (either in raster formats or geometrical grids) where organisms move through each cell following one of the possible movement principles. Here the nodes are typically placed at the centroid of each cell and connected by edges to their adjacent neighbours, conforming a minimum planar graph (Urban et al. (2009)). Connectivity routes at a landscape scale can be carefully delineated, while also describing interactions at a local scale through clear cell-to-cell relationships (Cushman et al. (2013)), permitting the highest flexibility of movement, and being specially suitable representations in heterogeneous dispersal matrices (Wiegand et al. (1999)). As a matter of fact, Dunning et al. (1992) stated that *"a species abundance in a particular focal patch may be more strongly affected by characteristics of contiguous patches than by those of more distant parts of the landscape"*.

Several geometries can be used to form the grid, from the widely used rasters to hexagonal grids or Dirichlet tessellations. Connectivity is then examined at the scale of a single grid cell (Galpern et al. (2011)), but even though the principles for movement are the identical, the choice of the geometry can have a significant impact on the simulated dispersal behavior (Holland et al. (2007)). Moreover, these representations have a tendency to be more computationally demanding than patch-based alternatives, with grid resolution as a limiting factor for memory capacity and simulation speed (Cushman et al. (2013)).

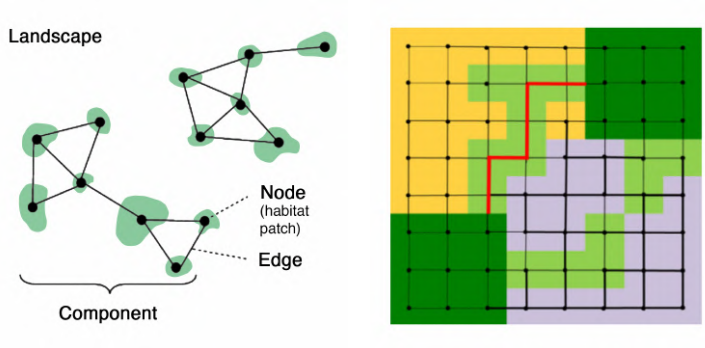

(a) Path-based representation (b) Grid representation

Figure 1.2. Landscape spatial representations.
Adapted from Kadoya (2009) (1.2(a)), Diniz et al. (2020) (1.2(b)).

1.1.4 Landscape connectivity models

Landscape connectivity can be assessed using a variety of methods, the choice among which is primarily determined by the objective of the study (Kool et al. (2013)). The two methods described hereafter are based on graph structures, with nodes representing landscape elements or spatial features to be connected, and links the cost or probability of connection related to the organism under consideration (Saura and Pascual-Hortal (2007)).

Models based on least-cost paths and centrality measures (Figure 1.3(a)) apply the concepts of network analysis to identify the locations of the cheapest routes (i.e., least-cost paths, with the minimum cumulative cost value), examine node importance through centrality measures (Estrada and Bodin (2008), Galpern et al. (2011), Diniz et al. (2020)), community detection, network cohesion, and node resilience via a set of metric-based analyses (Lookingbill and Minor (2017)). The main drawback of this method is that one can only identify the locations of the optimal routes as unambiguous corridors, without information on how cost values are distributed over the landscape, which may imply that very similar corridors that could be found elsewhere can go unnoticed (Cushman et al. (2013)).

Models based on circuit theory (Figure 1.3(b)) are also underlain by graph configurations but apply the electrical concepts of resistance, conductance, current and voltage in ecological connectivity. The network edges are here replaced by resistors (Diniz et al. (2020)) and, following Ohm's law, when a voltage is applied between two nodes in a resistive circuit, the total amount of current I that flows between them is defined in Equation 1.1 by the applied voltage V and the resistances R in the circuit (McRae et al. (2008a)). The lower the resistance (or the higher the conductance, its inverse), the greater the current flow.

$$I = \frac{V}{R} \tag{1.1}$$

One can also interpret currents as random walks, in which the probability that a random walker would move from a node along any graph edge is proportional to its conductance (McRae et al. (2008a)). Current density can therefore be used to identify ecological corridors. As a result, and advantage over least-cost analyses, using circuit-theory based models all movement routes are considered simultaneously, so we obtain a continuous current map that illustrates the probability of species movement through each cell of the landscape (Churko et al. (2020), McRae et al. (2008b)). However, the lack of metric-based analyses makes the distinction of important nodes and prioritization of locations much less evident.

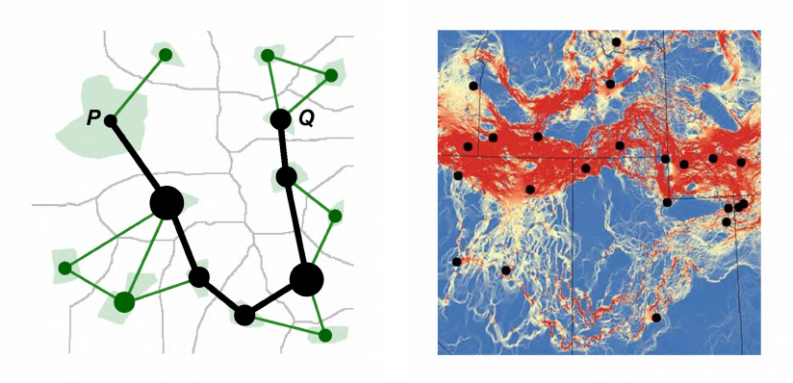

(a) Least-cost paths and centralities (b) Circuit theory-based

Figure 1.3. Landscape connectivity models.
Adapted from Chubaty et al. (2020) (1.3(a)), Carroll et al. (2012) (1.3(b)).

1.1.5 Landscape resistance to movement

The organism's willingness to transverse a certain landscape element is represented by the values of resistance to movement, which quantitatively estimate how environmental variables influence animal dispersal (Zeller et al. (2012)). In other words, *"resistance val-*

ues represent landscape features as the factor by which they may slow the movement of the organism" (Chubaty et al. (2020). Although one could understand resistance as the inverse of habitat suitability (Stevenson-Holt et al. (2014)), typically its estimation is done by means of resistance-value transformations from habitat suitability tiers or distributions (Keeley et al. (2016)). Churko et al. (2020), for instance, tested null, exponential, sigmoidal, logarithmic, and linear transformations to test different barrier effects of unsuitable habitats, Duflot et al. (2018) proposed a more accurate negative exponential transformation function from habitat suitability thresholds. Resistance values are represented in spatially explicit resistance layers (also referred as resistance maps or surfaces), typically consisting of raster grids that represent the cost of movement tailored to given species, which are then summarized as edge weights in the graph configurations (Cushman et al. (2013), Churko et al. (2020)). In least-cost path analyses, this translates into the cost of travelling through each cell (Singleton (2002)), while in circuit theory-based analyses reflects the relative probability of moving into each cell (McRae et al. (2008a)). Resistance layers can typically be obtained from two approaches:

Based on expert opinions: In this approach, experts are asked to rank each landscape feature, or sets of environmental variables, according to their permeability to movement for each species (Churko et al. (2020)). Compared to empirical approaches, resistance layers derived from expert opinions have been criticized due to the suboptimal parametrization of environmental factors (Zeller et al. (2012), Cushman et al. (2013)). Even though the controversy over its accuracy, this remains the most widely used method as empirical data is frequently missing (Duflot et al. (2018), Compton et al. (2007)).

Based on empirical models: These approaches rely on biological data, in most of the cases to produce habitat suitability and species distribution models, which take species observations in relation to ecological conditions to predict habitat preferences (Guerry and Hunter Jr (2002)). Other methods include mark-recapture and experimental movement studies, telemetry, and landscape genetics, which are rarely employed due to logistically complicated and time consuming processes (Cushman et al. (2013)).

1.1.6 Types of connectivity simulations

Movement routes are computed between selected start and end points, commonly called focal nodes (Anantharaman et al. (2020)). Depending on the placement of these nodes, connectivity models can lead to different results. In this regard, two types of connectivity can be distinguished:

Functional connectivity: In this type of simulation, the focal nodes are placed at specific species habitats, registered observations, protected areas, or some other locations representative of the species behaviour in the landscape. The goal of these simulations is to analyze realistic or potential movement patterns associated with the specific species ecological behaviour between focal points where the species is very likely present.

Structural connectivity: In this approach the focal nodes are randomly placed along the perimeter of the study area in order to characterize its potential landscape permeability, ignoring the present distributions of the species (Churko et al. (2020)). These models are usually easier to set up and provide a more general picture of how the arrangement of the landscape matrix shapes the movement potential (Hall et al. (2021)).

Concerning the number of species involved, connectivity maps can be:

Single-species: The simulations are tailored to individual species, with resistance maps representing their specific preference for different landscape elements. They typically constitute the basis of landscape connectivity assessments and usually performed for a set of species of interest.

Multi-species: These single-species maps including diverse movement ecologies can then be normalized and combined into a unique map that provides useful insights to improve landscape connectivity for all of the considered species (Churko et al. (2020)).

1.1.7 Tools for BGI and Ecosystem Services planning

Urban models and decision-support tools are attractive means of supporting the planning process as they provide virtual laboratories to allow planners and other stakeholders to test hypotheses and ideas that are important to their decision-making (Bach et al. (2020)).

Numerous models are today available, ranging from regional planning to urban environments. Many regional models including ecosystem services assessments (Grêt-Regamey et al. (2017)) are targeted to conservation and ressource management (e.g. Marxan (Ardron et al. (2008))); forest management (e.g. LANDIS-II (Scheller et al. (2007)) and FVS (Crookston and Dixon (2005))); or agriculture (e.g. Daisy (Hansen et al. (2012)) and CropSyst (Stöckle et al. (2003))). Some are also developed specifically for connectivity modeling, like Circuitscape (Anantharaman et al. (2020)) or the R package `grainscape` (Chubaty et al. (2020)). However, none of these mentioned models adequately represent urban space and, alone, miss important analyses for participatory and multi-criteria decision-making in cities.

In urban settings, the most used tools focus particularly in stormwater management (e.g., SWMM (Gironás et al. (2010)), EPANET (Rossman (1995)), or MUSIC (Wong et al. (2002))). Certainly, some have also broadly included biodiversity, like InVEST (Hamel et al. (2021)), through proxies of habitat suitability and distances between habitats, but don't support the functioning of ecological networks through informed connectivity modeling. In fact, there's no urban decision support tool, to date, able to integrate local and detailed landscape permeability while being grounded on movement behaviours at a landscape scale. As a matter of fact, urban biodiversity research is only just starting to catch up with a broader field of urban developments (Norton et al. (2016)).

Taking biodiversity into account in urban planning processes in a rigorous and detailed manner is extremely challenging for planners and land managers (Norton et al. (2016)), not only it is a broad and complex concept, but its scale-dependency makes it even harder (Savard et al. (2000)). Patch-based representations and delineation of least-cost paths may miss numerous feasible opportunities when considering multi-functionality constraints, and circuit theory grid-based approaches are too computationally demanding for alternative testing and exploratory modeling.

The Urban Biophysical Environments and Technologies Simulator (UrbanBEATS) is an integrated modeling tool designed to support the planning of sustainable, liveable and resilient cities (Bach et al. (2020)). Due to its underlying structure and core philosophy, this is the model used in this study as a reference for a potential integration of a biodiversity module. Its main objective is to investigate potential opportunities for Blue Green Systems, mapping urban characteristics through different types of networks, and including geopolitical information. UrbanBEATS provides the means of conducting extensively integrated studies, but also light-weight rapid assessments of specific aspects (e.g., pollution management, enhancing urban amenity). Any simulation should have clearly defined modelling aims, allowing for key modules to be selected and outputs to be generated in a time efficient manner without unnecessary information overload. To that aim, the model simplifies spatial representation through a grid structure using the concept of "blocks" to represent local neighbourhoods across the urban area. A block is the smallest spatially explicit unit in the model and contains rich information about the urban area, as a geodatabase of model information (Bach et al. (2020)).

1.2 The Swiss BGB Initiative and precedent research

The present study is framed within the Swiss Blue Green Biodiversity Research Initiative, an Eawag-WSL collaboration focusing on biodiversity at the interface of aquatic and terrestrial ecosystems. The study is itself a continuation of the research carried out by Donati et al. (2022) for the project *"Blue-green infrastructure for biodiversity enrichment in*

human-dominated landscapes", and is intended to serve as a link and transition towards the upcoming project *"BlueGreenNet: Social-ecological networks to enhance biodiversity in peri-urban regions"*. In their study, Donati et al. (2022) integrated biological and highly resolved urban-rural land-cover data, ensemble models of habitat suitability, and connectivity models based on circuit theory, to improve multi-scale and multi-species protection of core habitats and ecological corridors in the Swiss lowlands. Considering a broad spectrum of amphibian species, they identified distributions of amphibian biodiversity hotspots and landscape elements essential to amphibian movability at the regional scale. More over, their work highlights that cities can make a substantial contribution to wider landscape habitat connectivity, with nearly 15% of high current corridors overlapping urban areas.

1.3 Knowledge gaps

Although BGIs are experiencing a growing momentum, multi-functional BGI research is still at its early stages Donati et al. (2022). Opportunistic approaches in urban planning fail to include biodiversity strategically, due in part to the following reasons:

- Regional conservation models focus on the management of natural resources and do not adequately represent urban space. Thus, urban structures are not properly represented and BGI technologies often not incorporated.
- Urban planning models are currently inadequate to support BGI strategies to protect and enhance biodiversity, lacking key ecological connectivity information at local and landscape scales.
- Circuit theory-based approaches within high resolution grid representations are computationally very intense, making it unable to test different scenarios, which are crucial for decision-making processes; and patch-based models tend to oversimplify the analyses and could miss important information.
- Many connectivity methods have been developed, leading to confusion around circuit theory or patch-based network approaches, functional and structural choices, and spatial extent and resolutions.
- There is no integrated approach that uses these concepts for the prioritization of crucial areas to support the ecological networks.
- For all of the above, there is no adequate planning guidance for BGI applying fundamental landscape ecology concepts for biodiversity conservation and enhancement.

1.4 Aims and objectives

To address the aforementioned challenges, this study aims to simplify and integrate the merits of landscape ecology and regional biodiversity assessments with detailed urban structures for BGI planning. With the goal of optimizing computation times and encourage exploratory modeling, we will assess the performance of different spatial resolutions and representations to merge circuit theory and network analysis methods. Through this novel approach we intend to propose a methodology to identify top priority urban areas to enhance connectivity at multiple scales. Ultimately, our findings are aimed to guide the development of a biodiversity module in UrbanBEATS to enable strategical BGI implementation in urban settings.

2 Methodology

2.1 Study area

The study area covers a surface of 3'133 km^2 including the Cantons of Aargau (AG) and Zürich (ZH) in the Swiss lowlands, with altitudes ranging between 264 m and 1'212 m.a.s.l. The canton of Aargau (1'404 km^2) holds 213 municipalities, consisting in general of minor and scattered communities, and has a population density of 490 inhabitants/km^2, with its capital, Aarau, that is home to more than 21'700 people. On the other side, the Canton of Zürich (1'729 km^2) has a population density of 900 inhabitants/km^2 and includes 169 municipalities, some of which forming major urban agglomerations. The capital itself, Zürich, has a population of more than 434'300 inhabitants (Confederation Suisse (2020)). A 42.9% of the study area consists of meadows, pastures, and other agricultural land; forests occupy a 31.1%; urban settlements a 22.2% (12.2% consisting of impervious surfaces and 10% of urban green spaces); water bodies cover a 3.8%; with the last <1% corresponding to other landcovers, like wetlands, rocky surfaces, and rubble-sandy grounds. Regional parks, Ramsar and Emerald sites, alluvial zones, dry meadows, amphibian breeding sites of national importance, and Pro Natura sites, are some of the major ecological infrastructures (depicted in grey in Figure 2.1(c)) (Donati et al. (2022)).

(a) Ortophoto and Canton boundaries

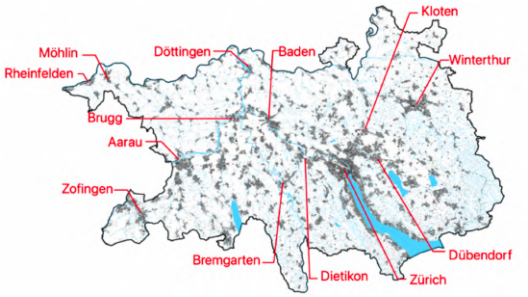

(b) Major urban settlements

(c) Major rivers and lakes

Figure 2.1. Study area. Adapted from Donati et al. (2022).

2.2 Overview of the methodological approach

The concept of our multi-scale landscape connectivity approach for biodiversity enhancement through the planning of BGI in urban areas is shown in Figure 2.2. The framework integrates the precedent work carried out by Donati et al. (2022). Specifically, we integrate the ensemble models (EM) of species distribution (SDM) and the circuit theory-based connectivity modeling that they carried out for the same study area at 30 m raster resolution. In the present study we defined a new set of scenarios defined by various spatial resolutions and representations and we performed circuit theory-based functional connectivity modeling with coarser, less computationally demanding inputs. We then built graph structures based on the circuit current outputs to perform a wide range of network analyses focused at identifying connectivity backbones, assessing movement patterns at global and local scales, and identifying critical locations for connectivity support. Our approach then combines these metrics into an index of node prioritization representative of multi-scale ecological dispersal processes. We illustrate this procedure by selecting the three most important urban areas for biodiversity enhancement, where we perform high resolution structural connectivity modeling to assess the permeability of their surroundings, identify conflicts and opportunities for BGI implementation.

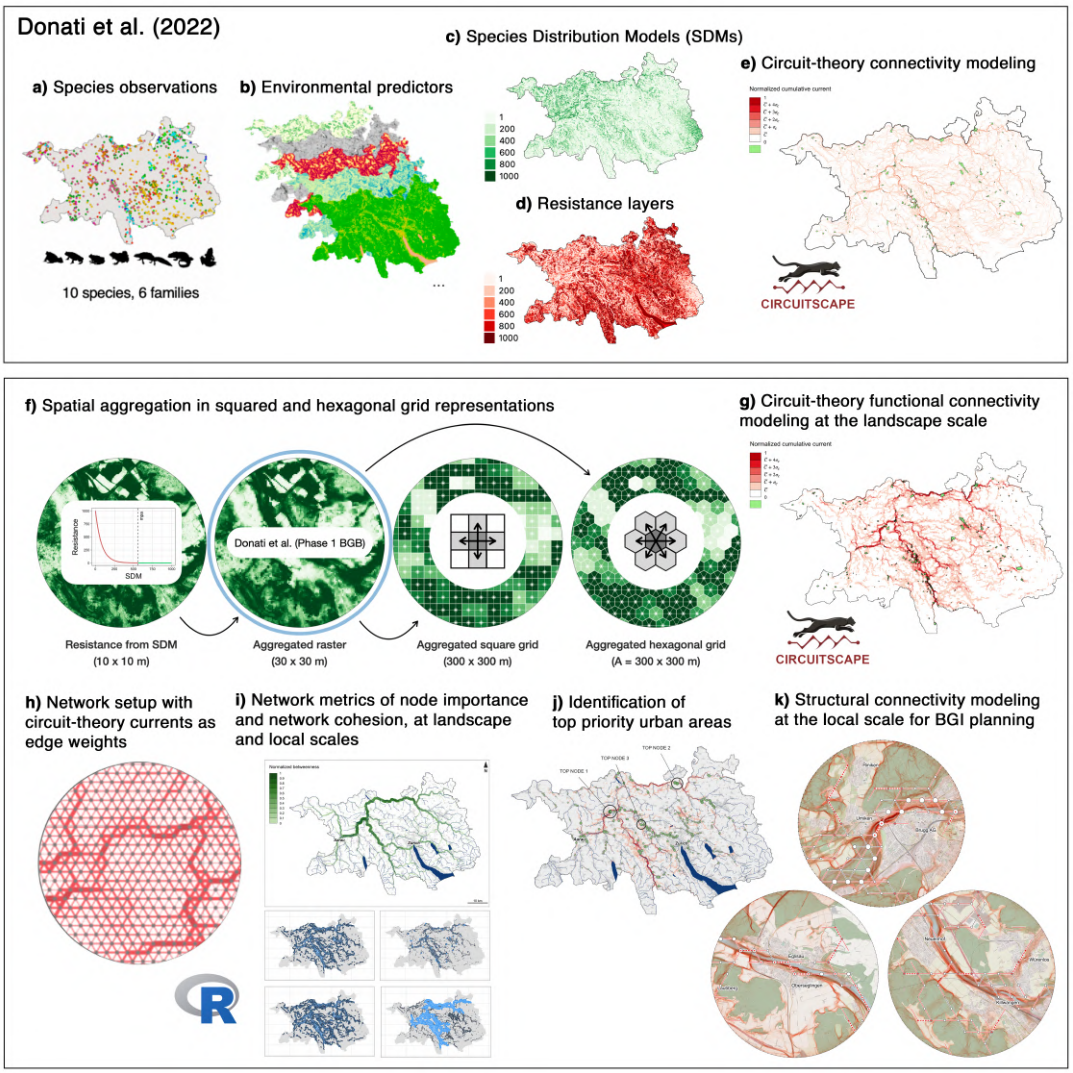

Figure 2.2. Overview of the methodological approach.

2.3 Amphibian species selection

As the connectivity of a certain landscape will be different for different organisms (Tischendorf and Fahrig (2000)), Donati et al. (2022) investigated 19 amphibian species and selected 10 of them using a multi-dimensional trait analysis (Villéger et al. (2008)). The authors used the Trochet et al. (2014) European database to compare the candidate species against six ecological life-history traits to cover all the possible trait diversity related to the amphibian dispersal, namely: the adult body size, metamorphosis size, parental care, egg/offspring number, juvenile diet composition, and displacement mode. Following the circuit theory-based connectivity analyses, they computed the correlations between the species-specific connectivity maps and found four different clusters describing different patterns of connectivity behaviours. In the present study, we used these results to select 4 species, one representative of each pattern of movement. For the specific choice we

also considered the phylogenetic tree of the Swiss amphibian species ((Pyron and Wiens (2011)), Donati et al. (2022)), such that the 4 chosen species would also pertain to different taxonomic families. Lastly, for groups in which there was still freedom of choice, we used the Swiss Red List of threatened amphibians (Schmidt and Zumbach (2005)) to base our last pick according to their protection status. The chosen species were: *Alytes obstetricans*, *Bombina variegata*, *Hyla arborea*, and *Salamandra salamandra*.

Species	**Family** (Pyron and Wiens (2011))	**Connectivity pattern** (Donati et al. (2022))	**Conservation status** (Schmidt and Zumbach (2005))
A. obstetricans	**Alytidae**	**3**	**Endangered (EN)**
B. variegata	**Bombinatoridae**	**4**	**Endangered (EN)**
Bufo bufo	Bufonidae	4	Vulnerable (VU)
H. arborea	**Hylidae**	**1**	**Endangered (EN)**
L. helveticus	Salamandridae	4	Vulnerable (VU)
L. vulgaris	Salamandridae	1	Endangered (EN)
I. alpestris	Salamandridae	4	Least Concern (LC)
R. temporaria	Ranidae	4	Least Concern (LC)
S. salamandra	**Salamandridae**	**2**	**Vulnerable (VU)**
T. cristatus	Salamandridae	1	Endangered (EN)

Table 2.1. Criteria for species choice. Selected species highlighted in bold.

***Alytes obstetricans* (Laurenti, 1768):** It breeds in various water bodies, ranging in size from a few meters to more than 1'000 m^2. It can live in both rich and poorly vegetated, sunny or shaded, cool waterways. When breeding, the toad heads for pools at the bottom of ditches and quarries, man-made ponds, water nets and other water bodies in alluvial areas, gullies in marshes, and even sheltered spots in streams and rivers. In most of the streams it frequents, the water flows all year round, so that some of the larvae can hibernate there. It prefers sunny slopes with sandy, loamy or aerated soil that is not very stable, but with sparse vegetation here and there. Walls exposed to the sun, with many cracks, piles of stones, or wood piles are ideal habitats. Ditches, open gardens, sunny forest edges, and extensive meadows can support toad populations during summer (Karch (2022)).

***Bombina variegata* (Linnaeus, 1758):** Its natural habitats are river valleys, meadows, marshes, wet forests and scree areas. In cultivated landscapes, it is nowadays found mainly in quarries, construction sites, and landfills with wetlands. Small, shallow, temperate water bodies are suitable for breeding. They can withstand a very high concentration of organic matter in the water, temperatures up to 36 ℃, and temporary drought. Suitable spawning sites should have water for at least 3 months in the summer, but dry out or be emptied annually. It avoids deep cold-water ponds that never dry out. Puddles of rainwater or stagnant water at the edge of flowing water, can serve as egg-laying sites. The terrestrial habitats must present a sufficiently wet soil all year long and sufficiently numerous hiding places. Field litter, dead wood, grass, and aerated forest floors are suitable habitats (Karch (2022)).

***Hyla arborea* (Linnaeus, 1758):** found in areas with several favorable water bodies and extensive, well-structured terrestrial habitats. Typical breeding sites are located in alluvial areas, low marshes, flooded meadows, and gravel and clay quarries. Favourable water bodies are shallow, exposed to the sun and have no inflow or outflow, which is why the water warms up faster. They spend most of its life on land and, during summer, they seek out a wind-sheltered, sunny spot with plenty of tall vegetation. A favorable terrestrial habitat must have a large food supply, be easily accessible and located no further than 1 km from the breeding water body. In winter, shelters in a place as protected as possible from frost and buries itself under moss, roots, stones or grass (Karch (2022)).

***Salamandra salamandra* (Linnaeus, 1758):** The forest is the typical habitat, with a preference for wet woodlands, where hiding places are more favorable. The larvae are deposited primarily in forest streams, more rarely in springs or small water bodies. If the species finds adequate conditions (streams and hiding places) in a built-up area, it can remain there permanently, even more than a kilometer from the nearest forest. The shelters used by the adults for the day are burrows of micro-mammals, rock cracks or caves of various sizes. In built-up areas, the salamander uses the crevices of stone walls, manholes and window wells as a daily refuge and wintering area. In streams, the larvae need areas with weak currents and rich shelters, under stones and dead leaves. The larvae remain most of the time under dead leaves or floating algae clusters. The overwintering site is usually a wet cavity protected from frost (Karch (2022)).

(a) *A. obstetricans* (b) *B. variegata* (c) *H. arborea* (d) *S. salamandra*

Figure 2.3. Selected amphibian species.

2.4 Species distribution models and habitat suitability

2.4.1 Ensemble models (EM)

The assessment of the distribution models for every selected species was carried out by Donati et al. (2022). The observations of amphibians were obtained from the Coordination Center for the Protection of Amphibians and Reptiles of Switzerland (Karch (2022)), including only the ones between 2017 and 2019 to account for the most recent distributions. To characterize the ecological niche in these observations, they used 13 amphibian whole-life cycle environmental predictors at a 10m resolution:

Variable type	Environmental predictors
Topography	Slope [º]
Hydrology	Nearest distance to water [m]
	Runoff coefficient [C]
Edaphology	Soil moisture variability
Vegetation	Median of the NDVI index (between 2016 and 2019)
	Standard deviation of the NDVI index (between 2016 and 2019)
	Median vegetation height [m]
Land use	Grassland density
	Urbanization (building density)
	Traffic intensity (vehicles/day)
Movement ecology	Nearest distance to forest [m]
	Nearest distance to a rock-gravel and sandy area (RGS) [m]
	Nearest distance to a road [m]

Table 2.2. Amphibian whole-life cycle environmental predictors used for the SDMs.

Ensemble modeling (EM) was used as the method of choice (Thuiller et al. (2016)). As an advantage over single model SDM techniques, EM uses various types of regression models to decrease the uncertainty and increase the accuracy of model predictors (Bolliger et al. (2017)). Donati et al. (2022) used a generalized additive model (GAM), a generalized boosting model (GBM), a generalized linear model (GLM), a random forest (RF), and maximum entropy model (Maxent). All models were evaluated for their accuracy using the areas under the curve (AUC) of the receiver operating characteristic (ROC) and the true skill statistic (TSS). To integrate model outputs and develop the EM predictions, each single distribution model was weighted according to its predictive accuracy. Projections of potential habitat were performed using the minimum predicted area threshold (mpa) for binarization (Préau et al. (2020)). The "mpa" threshold, computed with the `mpa.ecospat` function in the `ecospat` R package (Di Cola et al. (2017)), allows the removal of locations where habitat suitability values from the EMs outputs are lower than the suitability values of the bottom 10% of the species occurrence (Pearson et al. (2007)). The resulting SDM were then used to build up the resistance layers.

2.4.2 Landscape resistance to movement

The resistance layers were obtained using an exponential resistance-value transformation to the 10 m resolution SDM suitability maps. The transformation was done by means of the species-specific exponential decay function (Equation 2.1), proposed by Duflot et al. (2018), to strengthen the barrier effect of less favorable areas. The function uses the species-specific binarization threshold (mpa) (section 2.4.1) to assign the highest resistance value (R) of 1'000 when the habitat suitability from the SDM (SDM) is 0 (minimal), and a resistance value of 1 when the habitat suitability is equal or greater than the "mpa" binarization threshold.

$$\begin{cases} R = e^{\left(\frac{ln(0.001)}{\mathrm{mpa}} \cdot \mathrm{SDM}\right)} \cdot 10^3 & \text{if} \quad \mathrm{SDM} < \mathrm{mpa} \\ R = 1 & \text{if} \quad \mathrm{SDM} \geq \mathrm{mpa} \end{cases} \tag{2.1}$$

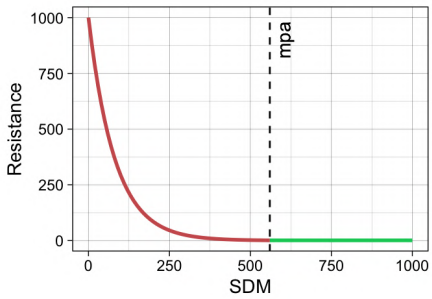

Figure 2.4. Example decay function for *Alytes obstetricans* (mpa = 560).

2.4.3 Spatial resolutions and representations

In order to reduce the computational demands for connectivity simulations to be carried out on computers within reach of most practitioners, and in order for the proposed methodology to be compatible with the "block" dimensions and core philosophy of UrbanBEATS (section 1.1.7; Bach et al. (2020)), we aggregated the resultant 10 m resolution resistance layers into squared and hexagonal spatial grids of an equivalent resolution of 100 x 100 m and 300 x 300 m using the median value. This statistic was chosen among other aggregation options (e.g., average) as it shows to be more robust against outliers.

As mentioned, two different geometries were chosen to build up the spatial grids. A square representation mimics the original raster layers, which is as well the most used framework for spatially explicit models and the way remotely sensed data is stored (Birch et al. (2007)). Additionally, we set up an hexagonal grid as it is considered to show more accurate movement patterns in connectivity modeling when compared to squared representations (Birch et al. (2007)). One reason is that hexagons are arranged on an equilateral triangular lat-

tice, which is the most compact arrangement of many equal circles Birch et al. (2007). Another major advantage is that each hexagonal cell has six adjacent nearest neighbours in symetrically equivalent positions (Birch et al. (2000)). In contrast, squared grids have two different kinds of nearest neighbours: orthogonal neighbours (i.e. von Neumann) sharing an edge, and diagonal neighbours (i.e., Moore) sharing only a corner Holland et al. (2007). The former type is incomplete, severely restricts movement directionality, and produces inconsistency as diagonal neighbours could be part of the same habitat or two fragmented ones. On the other hand, the Moore method introduces complications related to the unequal edge lengths and movements across vertices instead of sides (Childress et al. (1996)). Birch et al. (2007) stated that hexagonal geometries can perform substantially better than squares when modeling dispersal in coarse grids.

The resistance layers in a grid configuration where then converted into a spatial network structure, with nodes at the cell centroids and edges linking the adjacent neighbours sharing a side: four in the case of the squared grid, and six for the hexagons. The network data was then converted into an edgelist dataset with two columns indicating the pairwise connections (i.e., the IDs of the "from" and "to" nodes), and a third attribute indicating the resistance of the connection between the corresponding pair of nodes (i.e., the weight of the edge).

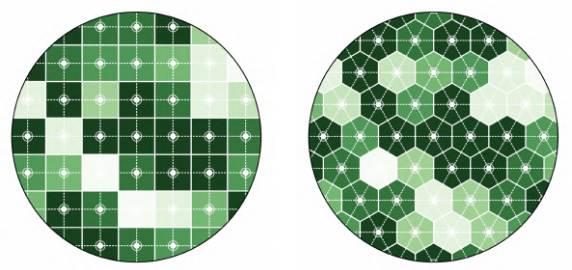

(a) *300 m squared grid* (b) *300 m hexagonal grid*

Figure 2.5. Spatial representations. Grid-based networks.

From	To	Resistance
1	2	663.09
1	13	695.78
1	14	709.80
...	...	...

Table 2.3. Edgelist network representation.

We then transformed the aggregated data in order to conserve the same ranges (i.e., minimum and maximum resistance values) than the original layers used by Donati et al. (2022). Finally, we computed the inverse of the resistance to obtain the conductance, required as an input for the circuit-theory based connectivity simulations (section 2.5).

2.5 Circuit theory-based functional connectivity modeling at the landscape scale

2.5.1 Single-species current maps

For the four species, we modeled circuit theory-based functional connectivity in Circuitscape's implementation in Python (version v4.0.5) (Anantharaman et al. (2020)). We performed 4 connectivity simulations per species, using the 100 and 300 m aggregated resistances, for both the squared and hexagonal grid representations. As focal nodes we used the 271 amphibian breeding sites of national importance to predict the maximum inter-breeding sites movement potential of amphibians across the study area (Donati et al. (2022)). The procedure to select the focal node IDs was the following: we first applied a buffer of a third of the edge length to the breeding sites polygons (for the 100 m resolutions that is 33 m in the square grids and 36 m for the hexagons, and in the 300 m resolutions 100 m and 107 m respectively) to include the cells whose centroids would fall outside the breeding site perimeter but still with a significant part of the cell inside (this was specially useful in small or thin and irregular breeding sites, where almost any centroid would happen to be inside the feature itself); we then performed an overlap analysis to select the nodes falling inside the buffered breeding sites, and finally we converted the selection to a dataframe containing the node (i.e., cell centroids) IDs: the second required input in Circuitscape. Tests with were also performed with buffers of half of the edge lengths, however this option was not picked as it included a significantly higher amount of nodes, slowing down the simulations considerably. With a third of the edge length all breeding sites were represented at least by one node.

We set up a pairwise calculation mode in a network data type format for the 100 and 300 m aggregated squared and hexagonal grid representations of the resistances. As opposed to Donati et al. (2022), who used a all-to-one mode in raster format, we had to use pairwise calculations as it is the only supported mode for network (i.e., grid-based) representations in Circuitscape (Anantharaman et al. (2020)).

Listing 2.1. Specifications for the Circuitscape mode in the .ini files

```
1 [Circuitscape mode]
2 data_type = network
3 scenario = pairwise
```

In the pairwise mode, connectivity is calculated between all pairs of focal nodes. For each pair of focal nodes, one is connected to a 1-amp current source, and the other to ground. Effective resistances are calculated iteratively between all pairs of focal nodes, and cumulative current maps are produced (Anantharaman et al. (2020)). The output cumulative

current maps were normalized between 0 and 1 for further comparative analyses. The simulations at 100 m resolution turned out to be computationally unfeasible and were finally discarded.

2.5.2 Multi-species current maps

Following the aforementioned normalized cumulative current maps for every species, we added up the four of them for every spatial representation (i.e., squares and hexagons), to produce multispecies connectivity maps that account the unique movement ecology of each species (Churko et al. (2020)). This maps can already serve as a useful evaluation of connectivity, as shown by Donati et al. (2022) and many other case studies, to estimate which areas of the landscape are highly connected. However, it is still not possible to know what are the critical thresholds at which the landscape is aggregated, what nodes are most important for connectivity, how movement is influenced at a local scale, and ultimately which urban areas should be prioritized to implement BGI solutions to support the ecological connectivity network, reason why we proceed with a spatial network analysis.

2.6 Spatial network analysis

Similarly to Table 2.3, the raw Circuitscape outputs in network mode consist also of an edge list which attributes (i.e., edge weights) are now the computed currents instead of the resistances. The fact of having converted the spatial grid maps (originally aggregated from the finer resolution rasters) into a spatial network topology (recall section 2.4.3), allowed us to re-enter the raw Circuitscape results back to the spatial network in QGIS, opening up all the network analysis possibilities otherwise out of reach. In other words, this allowed us to merge the circuit-theory based connectivity results with the analyses typically carried out in patch-based models (section 1.1.4).

For the analyses we used the `sfnetworks` R package (Van der Meer et al. (2022)), which connects the functionalities of the `tidygraph` package (Pedersen (2020)) for network analysis and the `sf` package (Pebesma (2018)) for spatial data science.

Graph metrics are used by ecologists to quantify the connectivity of the network in several ways. Selecting a graph metric though presents a challenge to researchers, Galpern et al. (2011) counted more than forty metrics among the studies reviewed. Based on Kupfer (2012), Galpern et al. (2011), Estrada and Bodin (2008), and Minor and Urban (2008), in the present study we selected a representative set of metrics and classified them into: (a) those that characterize the overall graph connectivity, (b) those that assess node contribution to connectivity at the whole landscape scale, (c) those that assess node importance for connectivity at the local scale, and (d) those that assess the network cohesion.

2.6.1 Metrics of overall graph connectivity

The following metrics were chosen as descriptive measures of the network's connectivity.

Mean edge weight: Describes the general suitability of the landscape for species-specific movement. Is calculated as the sum of all edge weight attributes (i.e., cumulative current derived from circuit theory-based simulations) divided by the number of edges in the graph (Galpern et al. (2011)). The metric was computed using the `summarize` verb implemented in the `dplyr` R package (Wickham et al. (2021)).

Diameter: Measures the length of the longest shortest path between any two nodes in the graph (Bunn et al. (2000)). The higher the diameter, the slower is the movement through the network (Minor and Urban (2008)). The metric was computed with the `graph_diameter()` function originally introduced in the `igraph` R package (Csardi and Nepusz (2006)).

Characteristic path length (CPL): Measures the average shortest path length over the network and is representative of the ease to reach any node (Minor and Urban (2008)). The `graph_mean_dist()` function also originally from `igraph` (Csardi and Nepusz (2006)), was employed for its calculation.

Community detection: Assesses the community structure of the network. We used the Louvain method (Blondel et al. (2008)), that seeks to optimize modularity (i.e., the extent to which nodes exhibit clustering (Newman (2006))) as the algorithm progresses (Van der Meer et al. (2022)). Nodes inside a cluster, or community, are more strongly related than to nodes in other clusters, a higher number of communities is thus indicative of possible subpopulations. The function `group_louvain()` implemented in the `tidygraph` R package (Pedersen (2020)) was used for that aim.

2.6.2 Metrics of node contribution to connectivity at the landscape scale

The following metrics were chosen as descriptive measures of the network's connectivity.

Betweenness centrality: Measures how frequently a node lies on the shortest path between any two nodes in the whole graph (Luke (2015)). This centrality metric is based on the idea that node importance refers to its location in relation to the least-cost paths in the network (Kolaczyk and Csárdi (2014)). A node with a high betweenness has therefore a crucial function due to its position of control over the flow of information in the network. More importantly, the spatial distribution of nodes with high betweenness delineates the backbones for connectivity support. We computed this centrality metric with the `centrality_betweenness()` function, implemented in the `tidygraph` R package (Pedersen (2020)), and inside the `dplyr::mutate()`

verb (Wickham et al. (2021)) on the graph object. The betweenness centrality can be calculated as follows (Freeman (1977)):

$$C_B\left(n_i\right) = \sum_{j<k} \frac{g_{jk}\left(n_i\right)}{g_{jk}} \tag{2.2}$$

where $g_{jk}\left(n_i\right)$ is the total number of shortest paths between nodes j and k that pass through node n, and g_{jk} is the total number of shortest paths between j and k (regardless of whether or not they pass through n).

2.6.3 Edge thresholding experiments for ecological corridors' subsetting

As the entire landscape graph consists of a single component the nodes of which have all a degree of 6 (except the ones at the perimeter), the network metrics of node importance at the local scale, based on degree measurements or different components, required a pre-processing step to subset only the significant nodes for connectivity, i.e., the ecological corridors. This identification of high current corridors was estimated by an adaptation of the edge-thinning technique, originally described by Keitt et al. (1997). We designed a simple analysis in which edges below a certain threshold current (derived from the Circuitscape analyses) were removed, and a new network was constructed. The connected subgraphs were then identified. The number of components, the mean order (i.e., number of nodes) for each component, and the network diameter were (Brooks (2006)). The value of the threshold was then iteratively increased and the graph metrics recalculated until the entire system was aggregated in one single component, the original network. The threshold values were ploted against the mentioned metrics, and the critical threshold chosen to subset the ecological corridors was determined mathematically at the value associated with the highest connectivity change (Galpern et al. (2011)). Following the study by Elliot et al. (2014), we based our thresholds on the specific distribution of the data. In concrete, we iteratively subsetted the edges with a current (C) equal or higher than the mean current ($\overline{C}$) plus an increasing number ($x = [0, 4]$) of standard deviations (σ_c).

$$C \geq \overline{C} + x \cdot \sigma_c \tag{2.3}$$

This method, a part of being objective, based on ecological reasons, species-specific, and therefore coherent for comparisons, also showed much better agreement when applying it to Donati et al. (2022) connectivity maps for similarity testing, as opposed to the 90th quantile threshold that the authors applied in their study, which showed to be meaningless with the aggregated data we used.

2.6.4 Metrics of node importance at the local scale

Degree centrality: Measures the number of edges adjoining the the node, and is an indicator of accessibility (Kupfer (2012). Depending on the habitat quality, high degree nodes may be highly transited areas (Minor and Urban (2008)). The metric can be computed with the `centrality_degree()` function, implemented in the `tidygraph` R package (Pedersen (2020)), and inside the `dplyr::mutate()` verb (Wickham et al. (2021)) on the graph object.

Local clustering coefficient: Measures the average fraction of the node's neighbours that are connected to each other (Minor and Urban (2008)). Highly clustered nodes imply access to a fair amount of nearby nodes and facilitate organism dispersal (Bodin et al. (2006)). This method, introduced by Watts and Strogatz (1998), can be measured by examining the number of closed triangles the node is part of, calculated using the `local_triangles()` function in `tidygraph` (Pedersen (2020)), together with the node degree.

$$CC_i = \frac{2N_i}{k_i\left(k_i - 1\right)} \tag{2.4}$$

Where CC_i is the local clustering coefficient of node i, N_i is the number of triangles the node participates in, and k_i is the degree of node (Dáttilo and Rico-Gray (2018)).

Compartmentalization: Also known as connectivity correlation (Melián and Bascompte (2002)), measures the relationship between the node degree and the average node degree of its neighbours (Minor and Urban (2008)). It provides a characterization of the susceptibility of the network to perturbations. A high value of the metric indicates more resistance to fragmentation and higher robustness of the corridor (Melián and Bascompte (2002)).

Component's order: A component is set of nodes that are connected to each other but separated from the rest of the network. Its order simply means the quantity of nodes that pertain to it. Therefore, the bigger the component the more nodes will be mutually reachable (Minor and Urban (2008)). The metric was firstly computed using the `group_component()` function of the `tidygraph` package, which assigns a component index to the nodes, we then grouped the nodes by component index and used the `length()` function to find out the number of nodes with the same component index.

2.6.5 Metrics of network cohesion

Additionally to the metrics of graph connectivity and node importance, we characterized the network cohesion of the ecological corridors subset through two different methods: minimum spanning trees and cut-nodes and edges.

Minimum Spanning Trees (MST) are tree structures in the network by which all nodes are completely connected with the minimum number of edges and the minimum total cost (Jalali et al. (2016)). This method can be used to identify the arterial corridors (Luo and Wu (2021)), and is therefore important in maintaining regional ecological integrity (Zhao et al. (2019)). The computation of the MST is a combinational optimization problem (Bazlamaçcı and Hindi (2001)). We used the `mst()` function from the `igraph` R package (Csardi and Nepusz (2006)), and using the Prim's algorithm for weighted graphs (Prim (1957)).

Cut-nodes and cut-edges are nodes and edges that, if dropped, would fragment a connected (i.e., single-component) corridor into separate, disconnected, components (Luke (2015)). In many types of networks cut nodes and edges thus occupy critical locations to preserve connectivity (Van der Meer et al. (2022)). These points and links are therefore weak spots against disturbances, and the robustness (i.e., resilience) of the network connectivity depends directly on them (Albert et al. (2000)). The function `node_is_cut()` from the `tidygraph` R package (Pedersen (2020)) was used for identifying the cut nodes. The algorithm successively deletes each node of the network and calculates the number of components, if the number increases, the node under consideration is a cut node (Van der Meer et al. (2022)). From there, the network was morphed into a linegraph to identify the cut-edges.

2.7 Spatial congruence analysis

Before proposing any strategy for BGI planning, the results derived from the coarser resolutions and different spatial representations had to be validated with the 30 m raster results from Donati et al. (2022). We based our analysis on the multi-species scenarios, so first the Donati et al. (2022) multi-species cumulative current map at 30 m raster resolution, considering only the 4 selected species of the present study, had to be built (section 2.5.2) as our base case scenario.

In order for our results to be comparable between each other and to the base case, we interpolated the squared and hexagonal 300 m resolution nodes' spatial point data into a raster using the Inverse Distance Weightning (IDW) algorithm (Shepard (1968)) with a power parameter $p = 2$ and an output raster cell resolution of 30 m. The function `idw()`

from the `spatstat` R package (Baddeley et al. (2015)) was used. The reason of choice of this method among other interpolation algorithms (e.g., krigging), was the dense and evenly distributed point data over the study area. With our 300 m results interpolated to 30 m rasters we were then able to calculate the spatial correlation between layers using the Spearman's rank correlation coefficient (ρ_s). Spatial correlations were computed with the `rasterCorrelation()` function implemented in the `spatialEco` R package (Evans (2021)). The Kendall correlation coefficient was also considered but avoided due to its computational complexity $O(n^2)$ (where n is the sample size), as opposed to Spearman's $O(n \log n)$ (Weichao et al. (2010)). Based on Akoglu (2018), we set our interpretation cut-points as follows:

Correlation coefficient (ρ_s)	Interpretation
0	Null
(0, 0.25]	Weak
(0.25, 0.5]	Moderate
(0.5, 0.75]	Strong
(0.75, 1)	Very strong
1	Perfect

Table 2.4. Interpretation of the correlation coefficients.

2.7.1 Validation of the aggregated resolutions

In this case, the IDW interpolation was done with the circuit theory-based cumulative currents as node (i.e., cell centroid points) attributes, obtaining 30 m resolution current rasters derived from the 300 m squared and hexagonal grids. We were then able to assess the the cumulative currents' spatial configurations of our coarser resolution results for validation. The [*multi-species 300 m square grid current*] and the [*multi-species 300 m hexagonal grid current*] were compared against [*Donati et al. (2022) multi-species 30 m raster current*] and against each other. For this analysis, we considered "strong" to "perfect" correlations as the criteria for acceptance.

2.7.2 Validation of the squared and hexagonal spatial representations

Ideally, the currents derived from the coarser resolution squared and hexagonal grids would be in agreement with the base case and with each other. Even if so, the two different representations could perform very differently in terms of the network analyses due to the different number of nearest neighbours (i.e., connections) of the squared and hexagonal grid cells (section 2.4.3). The goal of the analysis was to prove the better performance of hexagonal grids for the ecological network analysis. As hexagonal grids have a 50% higher number of connections, and therefore an increased choice of movement directions

than the Neumann squares, the hexagonal grid results were now considered as the base case scenario. We therefore proceeded to analyze the correlations between their network metrics. To maintain the coherence with the previous analysis we also computed the same IDW interpolation, now using the betweenness centrality as point attributes and obtaining 30 m resolution rasters of betweenness centrality. Betweenness was chosen among other metrics as it is the only node-specific metric that analyzes connectivity over the whole study area. Moreover, according to Ray and Burgman (2006) and McNeil et al. (2006), the calculation of the shortest paths (the basis of betweenness) is most likely to benefit from a change from a rectangular to an hexagonal grid. The comparison was performed between the interpolated 30 m rasters of the [*multi-species 300 m square grid betweenness*] and the [*multi-species 300 m hexagonal grid betweenness*]. Here, in order not to drag bias, we only considered a "very strong" to "perfect" correlation as the criteria for acceptance.

2.8 Analysis of BGI opportunities in human-dominated landscapes

2.8.1 Node importance for multi-scale connectivity support

Once the data was validated, we aggregated the network metrics into an index for the identification of the most relevant nodes for connectivity. To this aim, some indexes have previously been developed (Pascual-Hortal and Saura (2006), Saura and Pascual-Hortal (2007), Villéger et al. (2008)), yet they are all meant to be applied in patch-based graphs and not applicable to grid-based networks.

In the present study we propose a weighted combination of the node metrics of connectivity at both the landscape scale and at the local scale. For the assignation of the weights we first computed the Spearman's correlogram between the metrics and performed a cluster analysis to find groups of highly correlated variables. For that purpose, we used the Ward's Minimum Variance Clustering method, which defines the clusters in such a way that the within-group sum of squares is minimized (Borcard et al. (2018)). First we computed all the pairwise dissimilarities (distances) between the metrics using the Gower (1971) general dissimilarity coefficient within the `daisy()` function implemented in the `cluster` R package (Maechler et al. (2021)). This algorithm was chosen as it first standarizes all the variables into the same interval and has the capability of handling mixed data types. Next, based on these dissimilarities, we performed the hierarchical cluster analysis using the Murtagh and Legendre (2014) criterion in the `hclust()` function, from which we obtained the clustering dendrogram. To decide on the cutting level of the dendrogram we based our choice on both its direct interpretation and the graph of fusion levels, which plots the values where a fusion between two branches of a dendrogram occurs (Borcard et al. (2018)). The cutting

height was then set at the largest dendrogram branch and fusion level. This cluster analysis was then used to assign equal weights to every cluster of metrics, as opposed to a simple average between all of them. This way we were able to mitigate the correlation effects between metrics and avoid the over weighting of certain ecological aspects that could be explained by more than a single metric. Finally, the index was computed for every node as a measure of importance to support both the global and local connectivity.

2.8.2 Priorization of urban areas for BGI implementation

Reiterating the need to establish priorities given the resource constraints, stakeholder and implementation complexity, and the urgency to tackle biodiversity loss, we proceeded to select only the cut nodes. These nodes (recall from section 2.6.5), have a critical role in the resilience of the network and maintenance of the functional connectivity. We then proceeded to the calculation of the majoritary land-use in every node's grid cell, by using the mode statistic, to subset only those nodes located in human-dominated landscapes, concretely the land-use categories 1 to 12 from the UrbanBEATS classification (Bach et al. (2015)). The higher the computed rank in nodes under consideration, the higher the priority for BGI implementation.

2.8.3 Structural connectivity modeling at top priority urban areas

The subsequent step in the definition of more concrete considerations for BGI planning, consists in zooming in at the top ranked nodes. Structural connectivity modeling comes now as a great approach to assess the permeability of the areas that, at this step, have already been identified as the most crucial ones for biodiversity conservation and landscape connectivity support at the global and local scales. To illustrate the procedure we selected the top 3 ranked nodes. We first applied a 2000 m buffer at the nodes' point features to capture the surroundings over an area of 12.5 km^2. This distance was picked because the diameter of the buffer circle (4000 m), is the maximum dispersal distance of *Hyla arborea* (Trochet et al. (2014)), the species with the highest dispersal distance among the selected ones. Moreover, is an area big enough to include representative urban structures and landscape features, while being relatively small to allow for detailed computations.

The structural connectivity modeling was carried out using the original 10 m resolution resistance layers derived from the SDMs (section 2.4.2). That is the highest possible resolution based on the SDM inputs, 3 times more detailed than the simulations by Donati et al. (2022), which could only be handled by high performance cluster computing. A total of 126 focal nodes were placed every 100 m along the perimeter and circuit theory-based connectivity was modeled in Circuitscape, now using raster format inputs. The simulations were carried out for every species and then added up into multi-species current maps.

2.8.4 Environmental considerations for BGI design

The SDMs of Donati et al. (2022) entailed valuable data to support specific BGI solutions. We gathered the 13 environmental variables (Table **??**) and extracted their median values at the highest current cells inside the ecological corridors. The selection of these cells was done by further restricting the edge threshold by two additional standard deviations than in section 2.6.3). We observed the ranges and distributions of the variables and computed the peak values of the density distributions as the most preferred value of every variable. These "optimal" values where then compared to the median value at the grid cells of our top priority nodes. Large differences of the later with respect the most preferred values could provide an informed context to implement specific measures to increase the habitat suitability of the area.

3 Results and discussion

3.1 Overview of the simulation setups and computation times

In order to minimize the computational time while maximizing the quality of our outputs, we tested several spatial resolutions and representations (section 2.4.3). The simulations based on spatial grids featuring a 100 x 100 m cell area were rejected as they proved to be not feasible to run in the absence of high performance cluster computing infrastructure, with expected running times exceeding 49 days. As for the 300 m squares and hexagons, while both scenarios had almost the exact same number of nodes, the number of edges of the hexagonal grid-based networks was 50% higher than the reference squared-grid. The number of focal nodes and focal pairs was also higher, though in a lesser extent. In spite of this significant increase in the amount of information (an accumulated +58.52%), the running times only took, on average, 12.5% longer than the squared grids, making it safe to say that the hexagonal representation provided a much better input quality over computation time ratio, a non-negligeable benefit when using fairly coarse resolutions. This can be appreciated in the outputs showing more diverse and accurate flow directionality.

Scenario	Number of nodes	Number of edges	Number of focal nodes	Number of focal pairs	Computation time (average)
Squared grid 300 m	35'800	70'673	860	368'511	20h 02min
Hexagonal grid 300 m	35'753	105'717	885	391'170	22h 32min
Difference	-0.13 %	+49.59 %	+2.91 %	+6.15 %	+12.50 %

Table 3.1. Overview of the input qualities and average computation times.

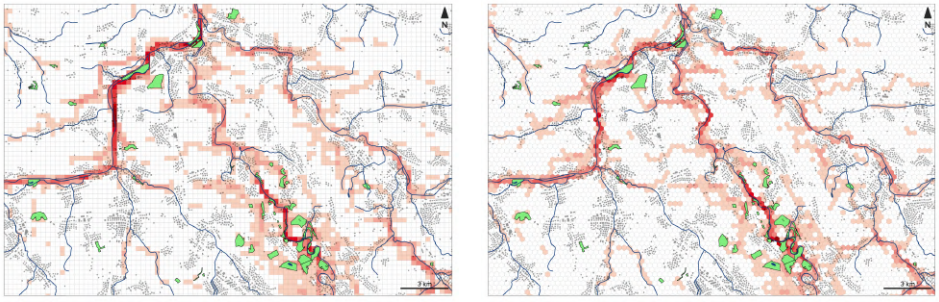

(a) Squared grid 300 m (b) Hexagonal grid 300 m

Figure 3.1. Influence of spatial representations on the normalized cumulative current.

3.2 Circuit theory-based functional connectivity modeling at the landscape scale

The functional connectivity maps highlight high currents along the Reuss, the Aare and the Rhein. More diffuse corridors are found across the landscape, with significant variance between species. Our results coincide with Donati et al. (2022) and Clauzel and Godet (2020) in the identification of forest edges, soils with variable moisture, wet forest habitats, and riparian habitats as landscape elements particularly contributing to the regional connectivity of the species.

Alytes obstetricans seems to disperse broadly over Aargau, being favored by forest edges contributing to its dispersal, with less patent corridors in the surroundings of Zürich, which could explain the absence of observations in that area. *Bombina variegata* showed similar preference for the river network, yet more attached to it and showing less diffuse pathways. The dispersal of *Hyla arborea* seems to be more restricted, with narrow corridors along the Aare and the Reuss and at the shores of the Greifensee and Pfäffikersee, areas with variable soil moisture. Indeed Donati et al. (2022) stated that the species only occupies a 17.1% of its potential suitable habitat.*Salamandra salamandra* was the species with more predicted movement across artificial landscapes, with relatively high currents inside the Zürich agglomeration. Although the species is widespread over the study area, this has to be interpreted with caution as an indicator of potential movement. In fact, *Salamandra salamandra* is the species with the lowest dispersal capability (Trochet et al. (2014)) and its connectivity could be compromised in the long term if we fail in preserving its core habitats (Manenti et al. (2009)).

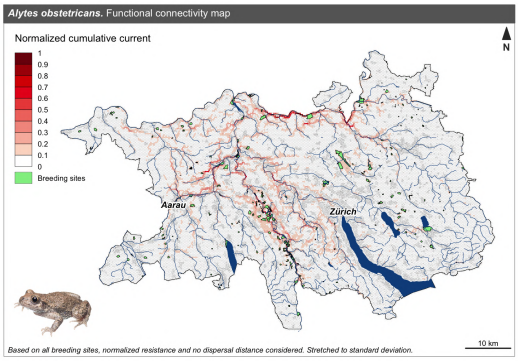

(a) *Alytes obstetricans*

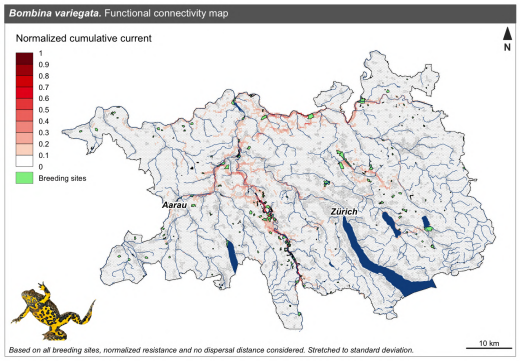

(b) *Bombina variegata*

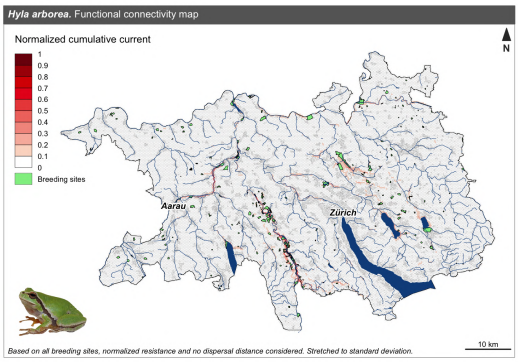

(c) *Hyla arborea*

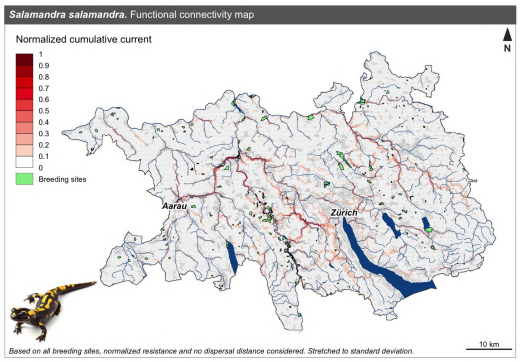

(d) *Salamandra salamandra*

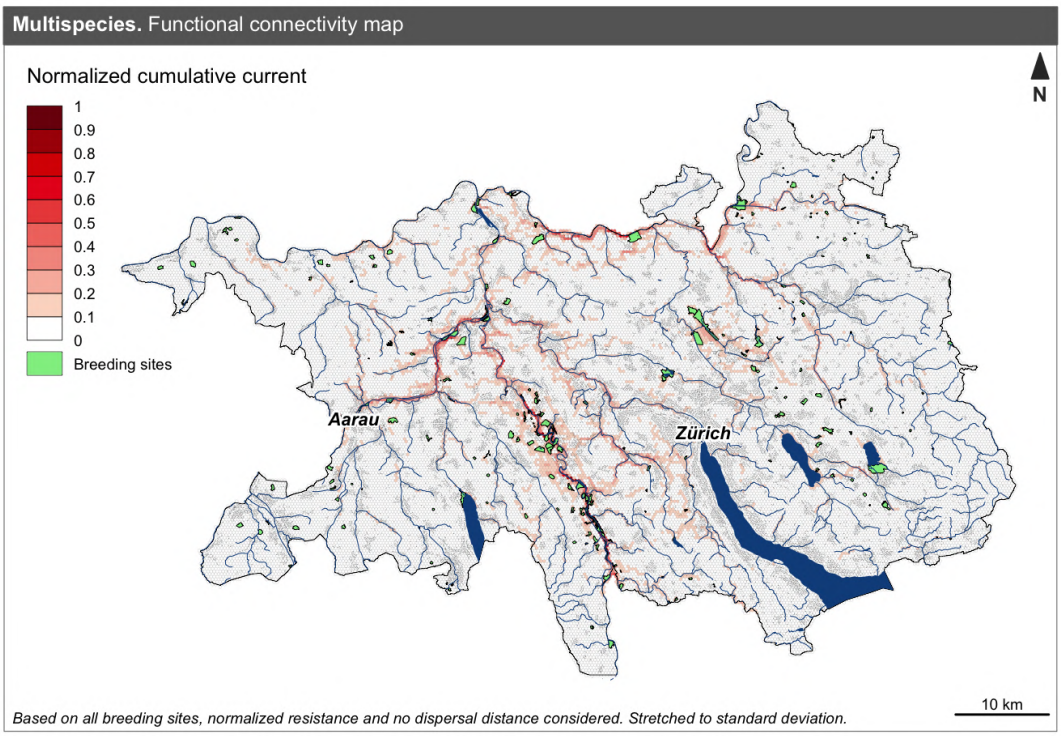

(e) Multispecies

Figure 3.2. Circuit theory-based functional connectivity modeling.

3.3 Spatial network analysis

3.3.1 Metrics of overall graph connectivity

The first network connectivity assessment was the computation of the overall graph connectivity metrics (section 2.6.1).

Scenario	Mean edge weight	Diameter	Characteristic path length (CPL)	Number of communities
A. obstetricans	0.0211	0.2767	110.654	57
B. variegata	0.0131	0.2182	110.654	59
H. arborea	0.0114	0.8639	110.654	59
S. salamandra	0.0158	1.0777	110.654	36
Multi-species	0.0199	1.3923	110.654	51

Table 3.2. Single- and multi-species metrics of overall graph connectivity.

According to the mean edge weight, *Hyla aborea* is the species that shows the least current intensity and therefore experiences the most difficulty in dispersal in this particular landscape. This can be related to the findings of Donati et al. (2022) about *Hyla aborea* exhibiting the narrowest and most scattered occupancy ranges. *Alytes obstetricans* showed the most favorable edge weights for dispersal, resulting in more diffuse corridors.

As shown by the network diameter, *Salamandra salamandra* experiences the slowest movement through the landscape network, closely followed by *Hyla arborea*, and far behind *Alytes obstetricans* and *Bombina variegata*. However, due to the relatively high mean edge weight, this could rather be explained by more complex movement patterns associated to terrestrial features. In fact, according to Donati et al. (2022), the distance to a forest and the runnoff coefficient are among the three most important variables for its habitat suitability.

Concerning the characteristic path length (CPL), we can compare the obtained metric of 110.654 with the value of 135.558 computed for the squared grid network. This higher value supports the fact that squared grid-based networks limit the mobility in a greater extent compared to hexagons, which traduces into higher difficulty to reach any node.

Lastly, all the species were classified into 57 to 59 communities (understood as groups of nodes of similar connectivity characteristics), except for *Salamandra salamandra* with only 36. This represents a smaller number of bigger clusters, which could mean that the landscape is conceived as less heterogeneous in terms of connectivity. Donati et al. (2022) found out that *Salamandra salamandra* is the most widespread species, even moving through artificial landscapes. In Figure 3.3, we can distinguish some groups of nodes covering big urban agglomerations (i.e., the Zürich and Winterthur areas), related to ecological infrastructure (i.e., the Jurapark Aargau) or sub-catchments (i.e., along the Reuss valley or the upstream basin of the Greifensee). The high number of communities of *Hyla arborea* can also explain its scattered populations.

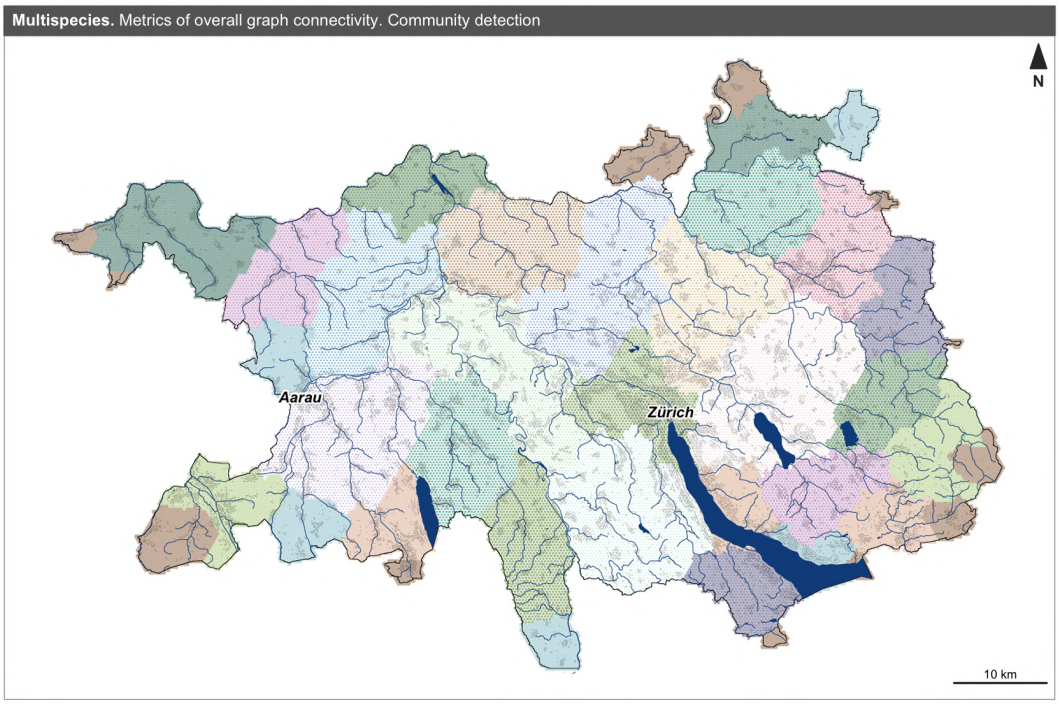

Figure 3.3. Metrics of overall graph connectivity. Multi-species community detection.

3.3.2 Metrics of node contribution to connectivity at the landscape scale

By computing the single- and multi-species betweenness centralities we identified the nodes located most frequently on the shortest path between any other two nodes in the network. The results highlight the most transited nodes and illustrate the backbones of the functional connectivity network (Figure 3.4). The rivers Reuss, Aare and Rhein are the main landscape features that support these routes, followed by the Töss and the Glatt. However, not all the backbone branches are associated to water features, specially the secondary ones. For instance, all species show a movement preference from the Reuss to the Zürich area, crossing through more terrestrial habitats towards the Limmat, like *Hyla arborea*, or the Zürichsee, like *Alytes obstetricans*, *Bombina variegata*, and*Salamandra salamandra*. On the multi-species map it can be observed a notable contribution of the cities of Zürich and Aarau to the backbone structure, highlighting the potential of urban areas to facilitate species dispersal.

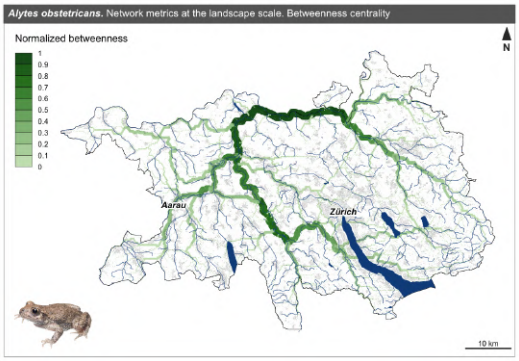

(a) *Alytes obstetricans*

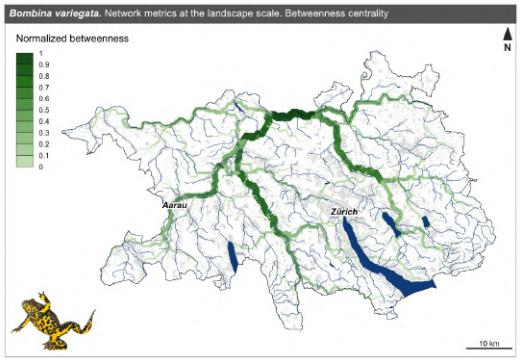

(b) *Bombina variegata*

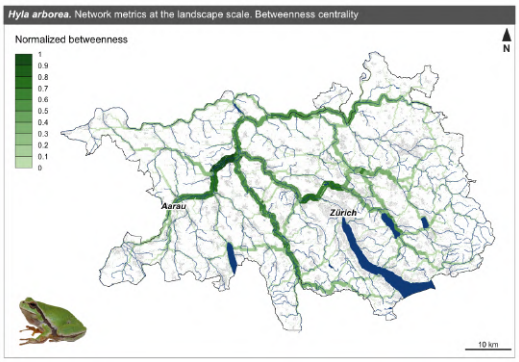

(c) *Hyla arborea*

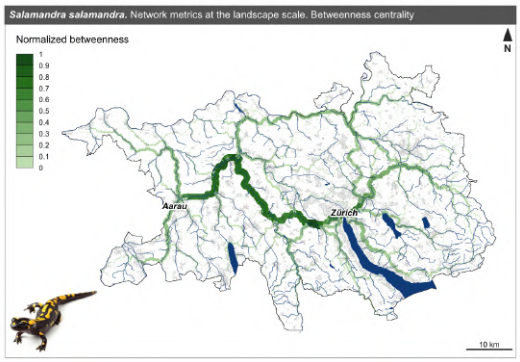

(d) *Salamandra salamandra*

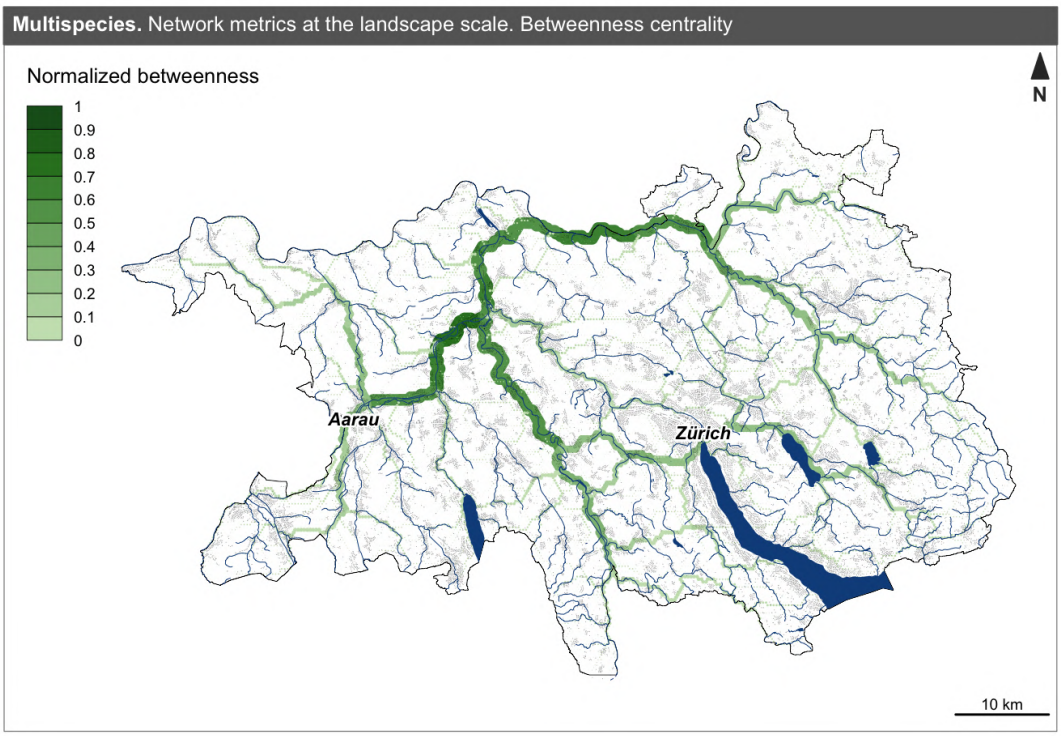

(e) Multispecies

Figure 3.4. Network metrics at the landscape scale. Betweenness centrality.

3.3.3 Edge thresholding experiments for ecological corridors' subsetting

As explained in section 2.6.3, we performed edge thinning experiments to decide on the most adequate and ecologically reasonable thresholds to subset the group of nodes and edges conforming high current ecological corridors. We carried out these tests for every species and the multi-species network. As presented in Figure 3.5, we found out an agreement between all the three assessed metrics on showing the greatest change in the connectivity at the threshold value that included only the edge currents equal or higher than the mean current plus one standard deviation ($C \geq \overline{C} + \sigma_c$). This was therefore the chosen threshold to subset the networks of the ecological corridors.

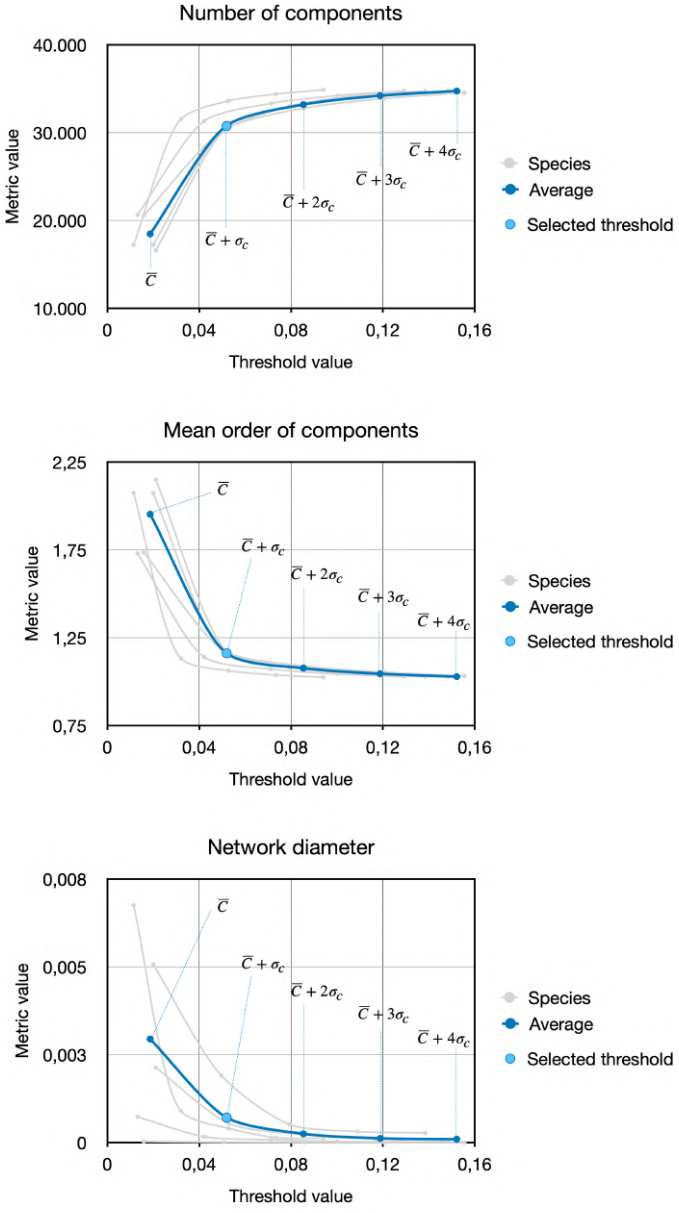

Figure 3.5. Edge thinning experiments. Evaluation of the network metrics.

3.3.4 Metrics of node importance at the local scale

Having obtained the ecological corridors network subset from the original single-component network with equal node degrees, we proceeded to compute the four local scale network metrics presented in section 2.6.4. Although having disaggregated the grid-based original network into multiple components, we still can observe some effects of the precedent topology, the most clear being the node degree and comparmentalization limited to 6 (i.e., the number of closest neighbours from each cell). From Figure 3.6 we can observe that the highest degree nodes are found inside thick corridors. The local clustering coefficient highlights closed triangles within thin and fragile corridors, where organisms can have access to an increased amount of nearby nodes. at the edges in fragile zones. Potentially highly transited and robust areas, characterized by high compartmentalization values, are found along the Aare, the Rhein, and the Reuss, specially downstream Bremgarten. Indeed, these three rivers, together with the Limmat, form the biggest connected component in the area, the rest being notably smaller.

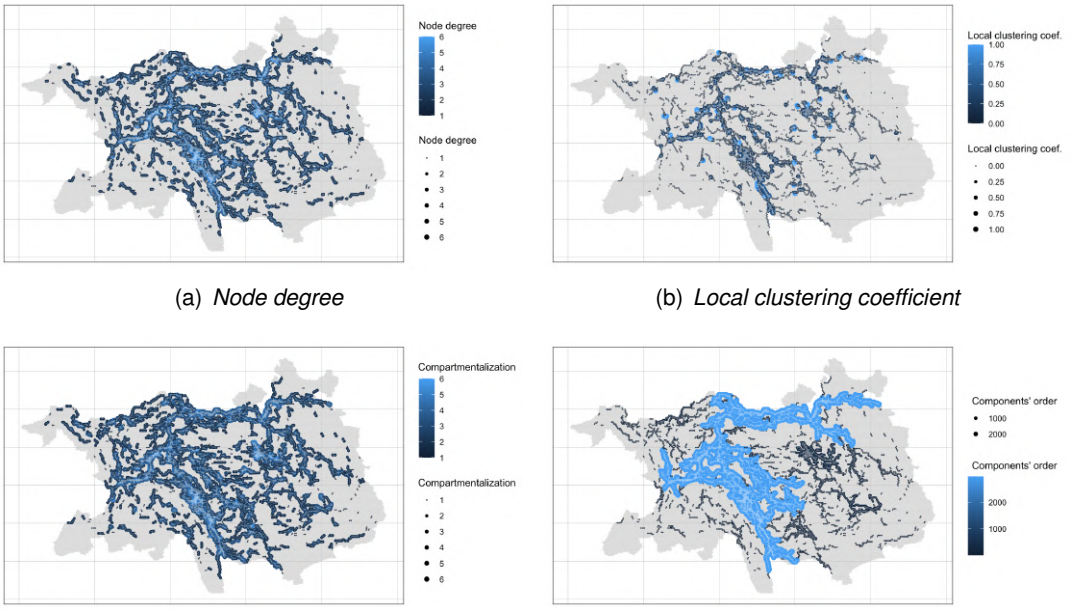

(a) *Node degree*

(b) *Local clustering coefficient*

(c) *Compartmentalization*

(d) *Components' order*

Figure 3.6. Metrics of node importance at the local scale.

3.3.5 Metrics of network cohesion

We used the ecological corridors network subset to identify cut-nodes, cut-edges, and compute the minimum spanning trees (MST) as described in section 2.6.5. In grid-based networks, minimum spanning trees cannot be meaningfully interpreted at the landscape scale, but can provide insightful indications at the local scale as shown in Figures 3.12 to

3.14. As for the cut-nodes and cut-edges, we computed their locations for every species and the multi-species scenario (Figure 3.7) and summarized them in the following table, were we compare the number of cut nodes (and cut-edges) with respect the total number of nodes (and edges) in order to relatively assess the fragility of the single and multi-species corridors to fragmentation. The higher this ratio, the higher the proportion of critical nodes where a perturbation to the connectivity would lead to the fragmentation into 2 disconnected components.

Scenario	**Nº of nodes** (in corridors)	**Nº of edges** (in corridors)	**Nº of cut nodes**	**Nº of cut edges**	**Cut nodes / nodes**	**Cut edges / edges**
A. obstetricans	5'272	5'984	2'257	1'415	0,43	0,24
B. variegata	4'743	5'639	1'793	1'146	0,38	0,20
H. arborea	4'585	5'182	2'006	1'318	0,44	0,25
S. salamandra	5'863	6'411	2'724	1'867	0,46	0,29
Multi-species	6'266	7'051	2'620	1'781	0,42	0,25

Table 3.3. Single- and multi-species metrics of network cohesion.

We identified *Salamandra salamandra* as the species with the highest proportion of critical nodes and edges, followed by *Hyla arborea*, *Alytes obstetricans*, and *Bombina variegata*. So, despite the high order of some of these corridors, the presence of almost half of them being critical nodes compromises their connectivity in the long term, with possible urban developments transforming the concerned land uses into barrier structures. Ideally these critical areas should be managed and protected against human-made impacts, promoting the restoration of its surroundings, and the creation of alternative corridors or stepping-stone habitats for redundancy (Grant et al. (2019)). In section 3.5 we will establish priorities to focus the planning efforts strategically.

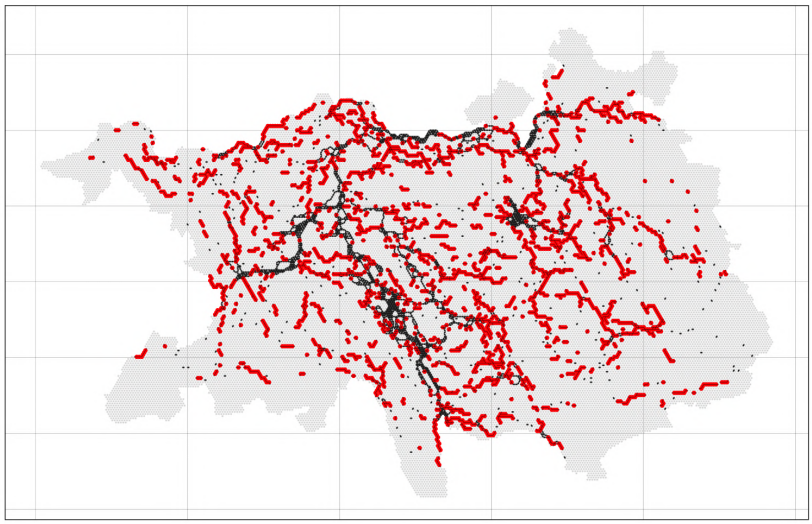

Figure 3.7. Cut-nodes (in red) of the multi-species ecological corridors.

3.4 Spatial congruence analysis

Our outputs were first visually compared to Donati et al. (2022) reference results (Appendix A), which were previously validated with overlaps with amphibian migration data. Additionally, we computed spatial correlations between the spatial layers. On the one hand we assessed the spatial congruency between our cumulative current results issued from the squared and hexagonal 300 m grids. These coarser setups showed to perform relatively well when compared to the reference 30 m rasters, showing Spearman correlation coefficients of nearly 0.7. Following the criteria on section 2.7, the 300 m resolutions were considered similar enough to the reference case and accepted for the analysis, specially considering the 'out of reach' computation infrastructure needed to obtain finer resolutions. The downside of coarsening the resolution was indeed much less severe than expected. Visually we could confirm mutual agreement in the location of high current corridors. On the other hand, we compared the performance of the two different spatial representations (i.e., squares and hexagons) in terms of the network metrics. Even though regarding the spatial distribution of the cumulative current there were almost no differences between the hexagonal and squared grids, with a nearly perfect correlation coefficient, the betweenness centrality metric showed to be significantly different. Due to their similar computation times, the 23.31% decrease in the correlation coefficient (from the circuit-theory similitude, to the network metrics) justified our choice to not consider the squared grid-based networks in the rest of the network analysis as the hexagonal grid proved to perform much better (section 3.1).

Node attribute	**Layer 1**	**Layer 2**	**Correlation coefficient (ρ_s)**	**Interpretation**
Circuit theory Normalized cumulative current	Raster 30 m (Donati et al. (2022))	Hexagons 300 m (node interpolation)	0.692	Strong (accepted)
	Raster 30 m (Donati et al. (2022))	Squares 300 m (node interpolation)	0.685	Strong (accepted)
	Hexagons 300 m (node interpolation)	Squares 300 m (node inyerpolation)	0.961	Very strong (accepted)
Network analysis Betweenness centrality	Hexagons 300 m (node interpolation)	Squares 300 m (node inyerpolation)	0.737	Strong (not accepted)

Table 3.4. Spatial congruence analysis. Spearman correlation coefficients between outputs.

3.5 Analysis of BGI opportunities in human-dominated landscapes

3.6 Priorization of urban areas for BGI implementation

Following the methodology described in section 2.8.2, we computed the correlations and pairwise dissimilarities between the metrics obtaining the hierarchical clustering dendrogram and the graph of fusion level values presented in Figure 3.8. From its interpretation, the best cutting level was found to be at a height of 0.6, obtaining two different clusters of similar metrics. Interestingly, one included the metrics of connectivity at the landscape scale (i.e., betweenness centrality), and the other grouped the metrics of connectivity at the local scale (i.e., node degree, local clustering coefficient, compartmentalization and component order). We considered the landscape and local scales of equal importance to connectivity. Hence, we assigned 50% of the weight to the landscape scale metrics and 50% to the ensemble of the metrics at the local scale, 12.5% to each one (Figure 3.9). Having previously normalized every metric between 0 and 1, we proceeded to compute their weighted average to obtain the index illustrating the priority rank of every node.

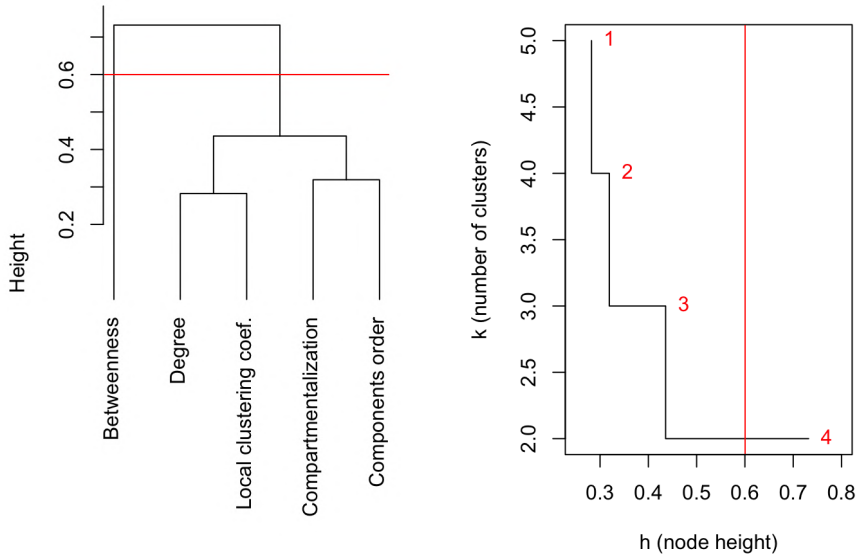

(a) Dendrogram (b) Graph of fusion level values

Figure 3.8. Hierarchical clustering analysis.

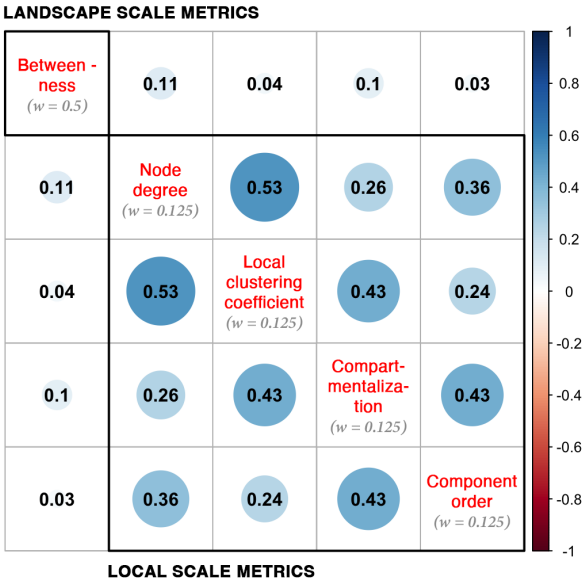

Figure 3.9. Spearman's correlogram, clusters of metrics and weighting factors.

We then attributed the priority rank to every cut-node and subset only the ones located in human-dominated landscapes (i.e., residential, commercial, mixed residential/commercial, industrial, municipal, transport, and open space land uses), potentially suitable for the implementation of urban or peri-urban BGI solutions (Figure 3.10). We then selected the 3 top ranked nodes as the most prioritary ones to support biodiversity.

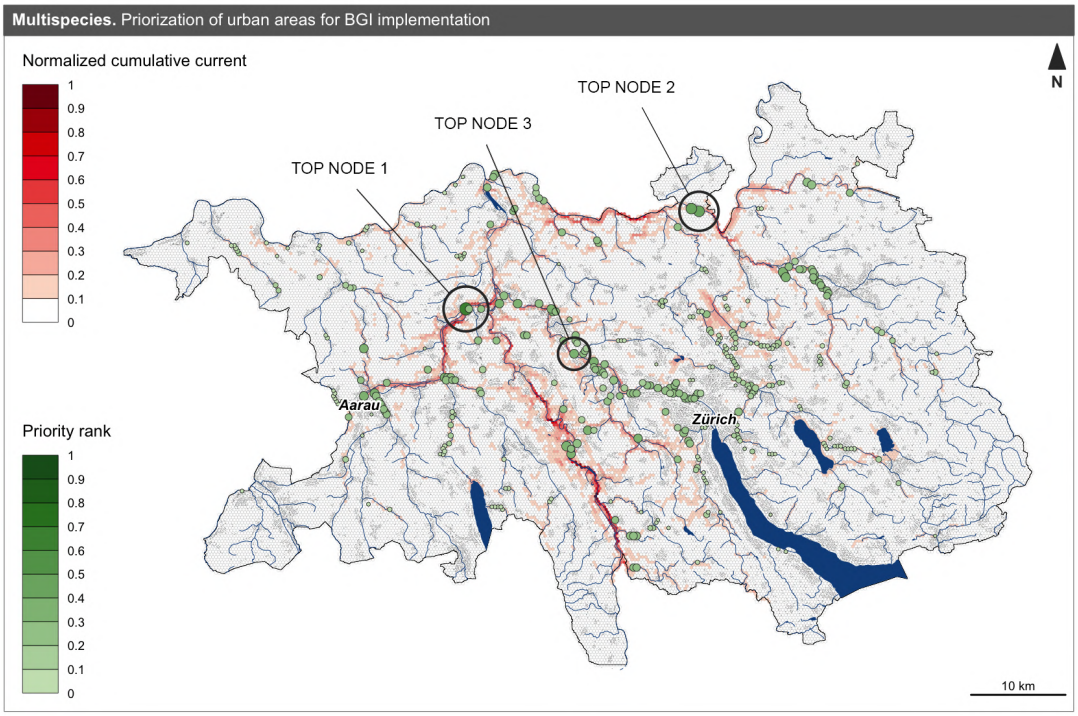

Figure 3.10. Priorization of urban areas for BGI implementation.

3.7 Local-scale planning of BGI

We modeled structural circuit theory-based connectivity at the surroundings of the three top priority nodes at a 10 m raster resolution. This allowed us to precisely assess the landscape permeability at the top priority areas identified through the functional connectivity analyses at the landscape scale, as described in section 2.8.3. Each simulation took 54 min on average, and allowed us to obtain three times finer results, at targeted locations, than Donati et al. (2022). We optimized time and resource management, in both computation and analysis, and rescinding the need of high performance cluster computing.

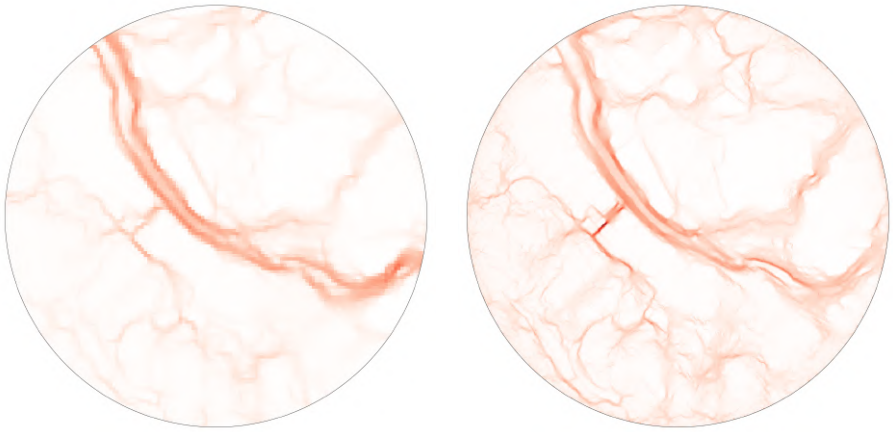

(a) Functional connectivity at 30 m resolution (b) Structural connectivity at 10 m resolution (Donati et al. (2022))

Figure 3.11. Comparison of 30 m and 10 m resolutions at top node 3.

Additionally, over the multi-species cumulative current maps we overlapped the ecological corridor networks illustrating the node metrics, minimum spanning trees and cut-nodes and -edges. Our maps highlight high resolution current corridors that can occur in particular streets, urban parks, small creeks or peri-urban aggricultural field edges. Moreover the network features indicate the contribution of those particular areas to the ecological connectivity at the landscape scale. All these spatial data was then represented over the OpenStreetMap (OpenStreetMap contributors (2022)) to identify possible conflicts with human-made infrastructures causing fragmentation.

A brief description of three top priority nodes is presented below.

3.7.1 Top node 1: Brugg AG

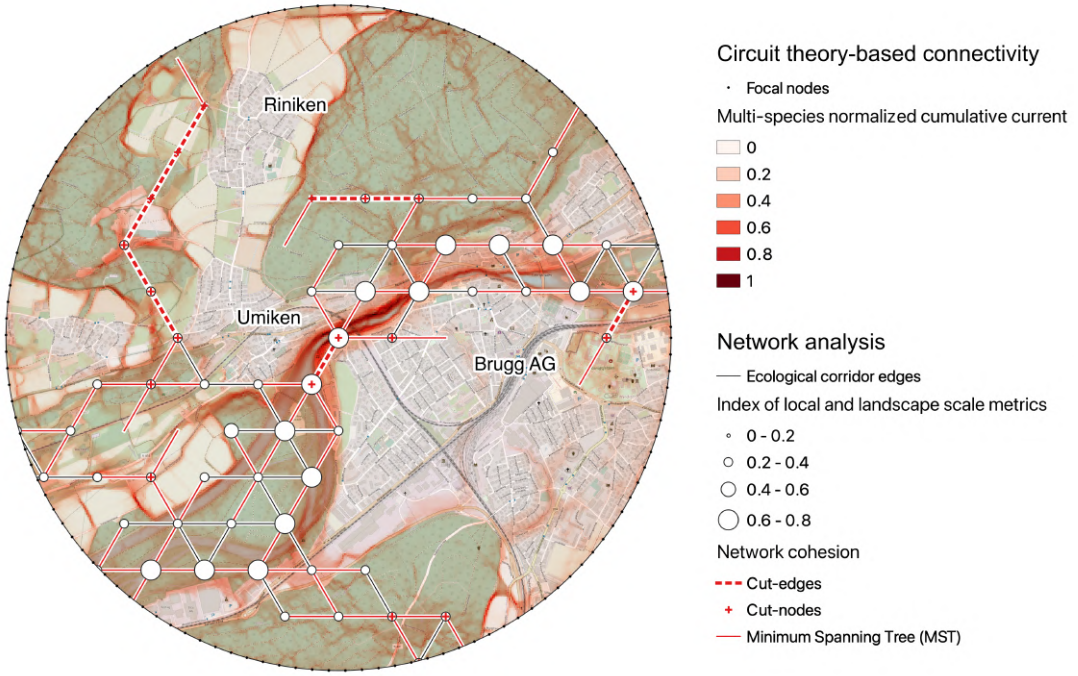

Figure 3.12. Top node 1.

The top priority area includes the municipalities of Brugg, Umiken and Riniken. Its high priority rank of 0.81 is in part due to its excellent contribution to the landscape scale functional connectivity, with a normalized betweenness value of 0.99. To minimize the impacts of fragmentation to the functional ecological network at the landscape scale, it is crucial to ensure movement permeability by creating additional corridors or stepping stone habitats, and removing all possible barriers. In this regard, the railway of the IR36 train is particularly conflicting, together with the urban areas of Brugg and Umiken. At the local scale, the contribution of this node to connectivity is also notable, with a node degree of 4, a normalized local clustering coefficient of 0.5, compartmentalization of 0.55, and being part of the biggest component of the ecological corridors. Concerning the permeability of movement, particularly high currents are found at the river banks of the Aare, hence BGI solutions should drive attention to the restoration of the river shores employing soft bioengineering techniques to provide heterogeneous micro-habitats while preventing excessive shear stress and erosion, specially at the outer side of the bend. Other corridors contributing to species movement at the region include forest edges at the interface with agricultural fields, and more diffuse corridors along green areas and urban creeks, like the Süssbach in Brugg.

3.7.2 Top node 2: Eglisau ZH

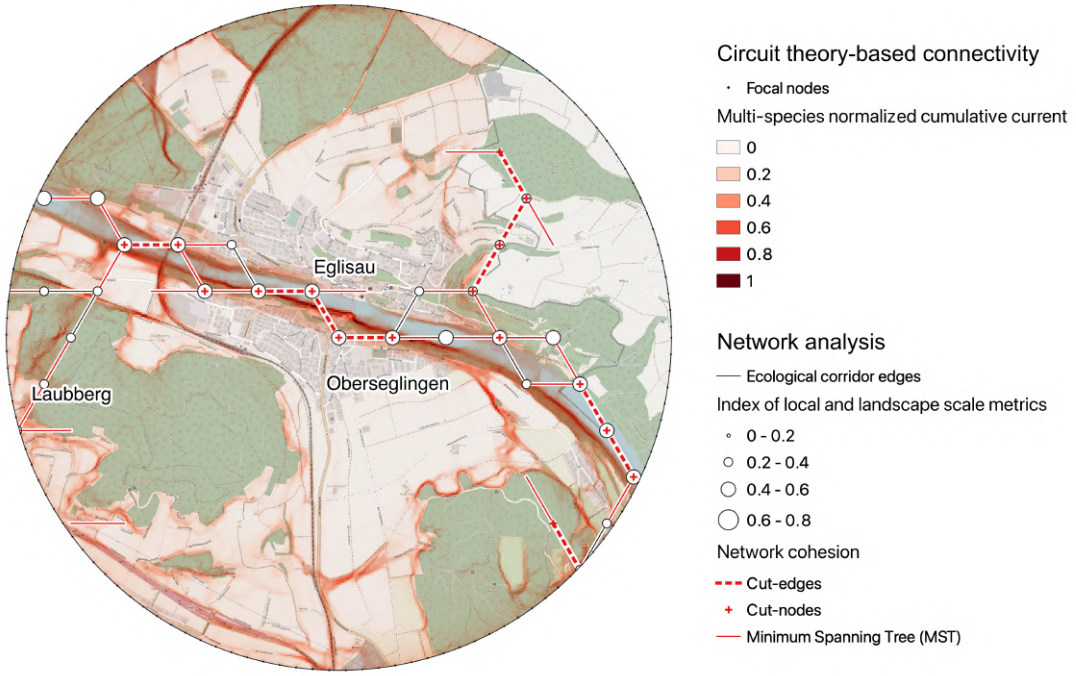

Figure 3.13. Top node 2.

The top priority node 2 is located at the municipalities of Eglisau and Oberseglingen. The importance of this node is mainly due to its contribution to the functional connectivity at the landscape scale, expressed by a normalized betweenness of 0.75, but not so much at the local scale. The current is concentrated into a narrow corridor along the Rhein with poorly access to nearby habitats, yet essential for species dispersal across the study area, even more considering the belonging of this node in the biggest corridor. In this case, the barrier effect of the railway is much smaller as it crosses the Rhein over a rather permeable viaduct, the Rheinviadukt Eglisau. However, the main road (Haupstrasse 4) bridge, crossing from Oberseglingen to Eglisau, has a much bigger barrier effect along the longitudinal connectivity of the right bank of the Rhein, a fragile sequence of cut-nodes and cut-edges with a critical function for biodiversity support. BGI solutions should specifically ensure a continuous corridor along the river banks combined with buffer zones between the urban area of Oberseglingen and the river.

3.7.3 Top node 3: Würenlos AG

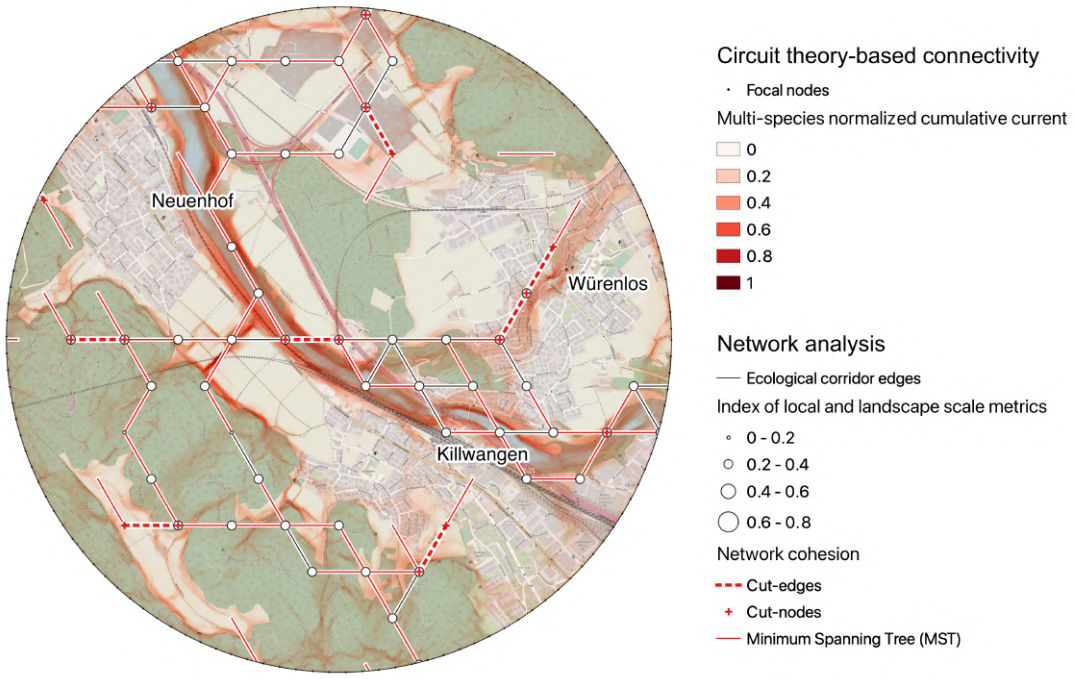

Figure 3.14. Top node 3.

The third top priority node is located between the municipalities of Würenlos, Killwangen and Neuenhof. This node is an example of a node with a lesser influence on the landscape scale connectivity, with a betweenness centrality of 0.12, but high connectivity potential at the local scale, as highlighted by a normalized local clustering coefficient of 1 and a compartmentalization of 0.64. Along the rather narrow corridors of the Limmat, this area benefits from the confluence of the Furtbach river, giving access to potential new habitats. An important conflicting infrastructure is the A3 highway and the service area of Würenlos (Fressbalken) at the immediacy of the confluence. From there, the Furtbach flows across the village of Würenlos, and outside the limits of the buffer its course is adjacent to the Otelfingen golf course, where it has recently been renaturalized and has access to multiple ponds and potentially favorable habitats compatible with human presence. Similar restoration measures could be implemented on its course through Würenlos, removing unnecessary impervious surfaces and replace the concrete river banks with green or mixed bioengineering techniques. Other secondary important corridors are found at the edges of Neuenhof and Killwangen forests and agricultural fields.

3.8 Environmental considerations for BGI design

By further restricting the edge threshold to the mean current plus three standard deviations, we extracted the environmental variables at the highest current corridors. Their ranges and distributions are presented in Figure 3.15. This procedure has been carried out for the 300 m hexagonal grid representation and the original 30 m rasters of Donati et al. (2022), as an additional method to compare the performance and spatial congruency of the different setups. As observed in the figure, both show very similar density distributions of the environmental variables, with almost a perfect agreement in their most preferred or "optimal" values (i.e., the peaks of the density distributions). This reaffirms the validity of the coarser resolutions, here in terms of the environmental descriptors of the ecological corridors.

This values can now be compared to the environmental characteristics at the top priority nodes, to target specific measures for habitat enhancement. To illustrate the procedure we examined the top node 1 (Appendix C) and we added the mean value of every variable in Figure 3.15 to analyze how far was this value from the optimal values representative of the highest current corridors. We observed fairly good agreement in the vegetation height, the distance to water, to forests, to roads and to rock-gravel-sand features. However, the NDVI index could be improved, as well as implementing specific BGI solutions to increase the soil moisture variability, decrease the runoff coefficient (i.e., remove impervious surfaces), and decrease the slope (i.e., restoration of the river banks with soft slopes and vegetated stabilization techniques). Some other values like the urbanization might be more difficult to modify, hence the importance of BGI to mitigate their negative effects.

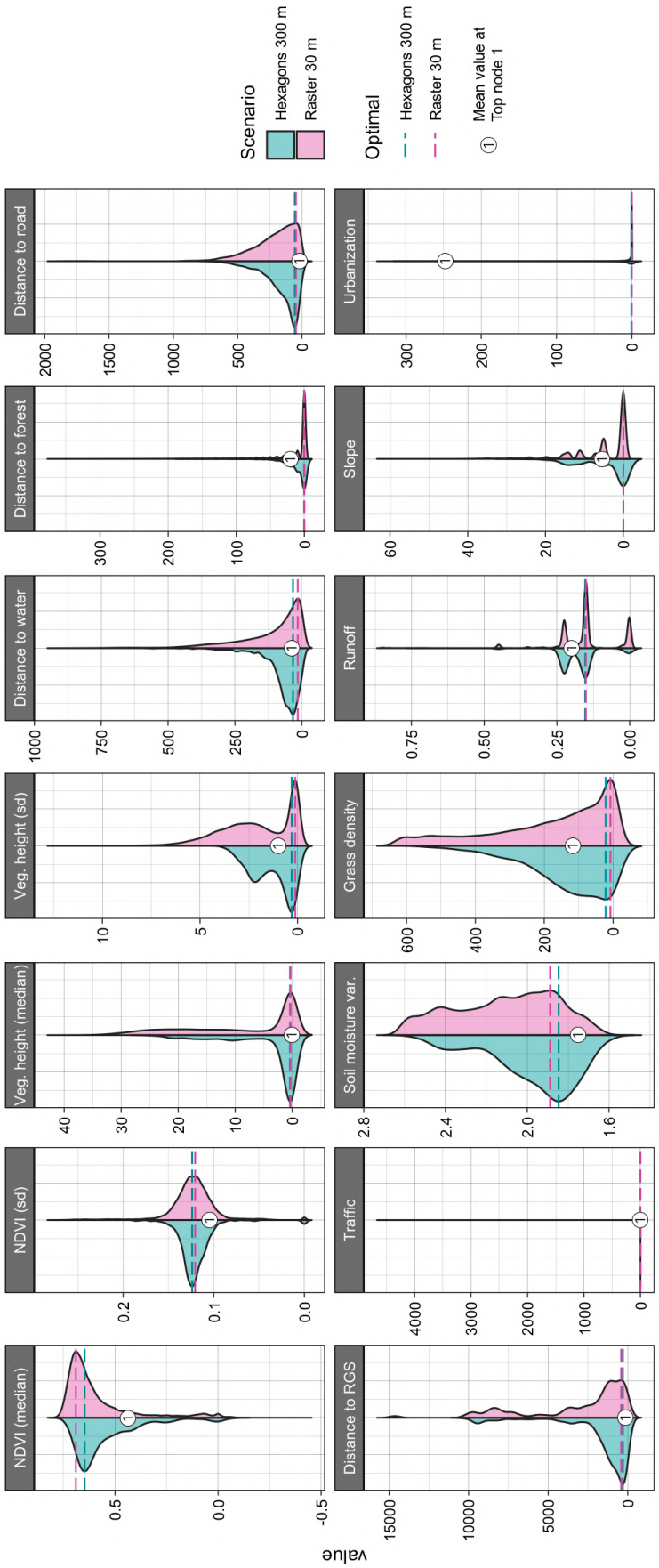

Figure 3.15. Environmental variable distributions at the highest current corridors, and mean variable values at the top node 1.

4 Conclusion

This research aimed to identify effective BGI planning strategies in urban areas for biodiversity enhancement. Based on circuit theory-based simulations and connectivity analysis using carefully selected network metrics, we have been able to identify critical locations for connectivity support and top priority locations for BGI implementation.

It can be concluded this novel approach succeeds on the simplification of circuit theory-based simulations by adopting alternative spatial representations and coarser resolutions based on the core phylosophy of UrbanBEATS, allowing for exploratory analysis to be carried out in a relatively short timeframe. Moreover, this approach strategically applies the concepts of functional and structural connectivity in different spatial scales and extents.

Looking ahead, these results have put in evidence the possibility to implement biodiversity in urban planning procedures and its implementation in UrbanBEATS will be developed in the upcoming months. Some improvements may include the consideration of species dispersal distances, and Dirichlet spatial representations, which will potentially better represent urban structures.

Bibliography

Akoglu, H. (2018). User's guide to correlation coefficients. *Turkish journal of emergency medicine*, 18(3):91–93.

Albert, R., Jeong, H., and Barabási, A.-L. (2000). Error and attack tolerance of complex networks. *nature*, 406(6794):378–382.

Anantharaman, R., Hall, K., Shah, V. B., and Edelman, A. (2020). Circuitscape in julia: High performance connectivity modelling to support conservation decisions. *Proceedings of the JuliaCon Conferences*, 1(1):58.

Ardron, J. A., Possingham, H. P., and Klein, C. J. (2008). Marxan good practices handbook. *Pacific Marine Analysis and Research Association, Vancouver*, page 149.

Bacchin, T., Ashley, R., Blecken, G.-T., Viklander, M., and Gersonius, B. (2016). Green-blue infrastructure for sustainable cities: Innovative socio-technical solutions bringing multifunctional value. In *9ème Conférence internationale sur les techniques et stratégies pour la gestion durable de l'Eau dans la Ville/9th International Conference on planning and technologies for sustainable management of Water in the City*. GRAIE, Lyon, France.

Bach, P. M., Kuller, M., McCarthy, D. T., and Deletic, A. (2020). A spatial planning-support system for generating decentralised urban stormwater management schemes. *Science of The Total Environment*, 726:138282.

Bach, P. M., Staalesen, S., McCarthy, D. T., and Deletic, A. (2015). Revisiting land use classification and spatial aggregation for modelling integrated urban water systems. *Landscape and Urban Planning*, 143:43–55.

Baddeley, A., Rubak, E., and Turner, R. (2015). *Spatial point patterns: methodology and applications with R*. CRC press.

Bazlamaçcı, C. F. and Hindi, K. S. (2001). Minimum-weight spanning tree algorithms a survey and empirical study. *Computers & Operations Research*, 28(8):767–785.

Beier, P., Penrod, K., Luke, C., Spencer, W., and Cabanero, C. (2006). South coast missing linkages: restoring connectivity to wildlands in the largest metropolitan area in the united states. *Connectivity conservation*, pages 555–586.

Birch, C. P., Oom, S. P., and Beecham, J. A. (2007). Rectangular and hexagonal grids used for observation, experiment and simulation in ecology. *Ecological modelling*, 206(3-4):347–359.

Birch, C. P., Vuichard, N., and Werkman, B. R. (2000). Modelling the effects of patch size on vegetation dynamics: Bracken [pteridium aquilinum (l.) kuhn] under grazing. *Annals of Botany*, 85:63–76.

Blondel, V. D., Guillaume, J.-L., Lambiotte, R., and Lefebvre, E. (2008). Fast unfolding of communities in large networks. *Journal of statistical mechanics: theory and experiment*, 2008(10):P10008.

Bodin, Ö., Tengö, M., Norman, A., Lundberg, J., and Elmqvist, T. (2006). The value of small size: loss of forest patches and ecological thresholds in southern madagascar. *Ecological applications*, 16(2):440–451.

Bolliger, J., Schmatz, D., Pazúr, R., Ostapowicz, K., and Psomas, A. (2017). Reconstructing forest-cover change in the swiss alps between 1880 and 2010 using ensemble modelling. *Regional Environmental Change*, 17(8):2265–2277.

Borcard, D., Gillet, F., and Legendre, P. (2018). *Numerical ecology with R*. Springer International Publishing, 2 edition.

Brooks, C. P. (2006). Quantifying population substructure: Extending the graph-theoretic approach. *Ecology*, 87(4):864–872.

Bunn, A. G., Urban, D. L., and Keitt, T. H. (2000). Landscape connectivity: a conservation application of graph theory. *Journal of environmental management*, 59(4):265–278.

Carroll, C., McRAE, B. H., and Brookes, A. (2012). Use of linkage mapping and centrality analysis across habitat gradients to conserve connectivity of gray wolf populations in western north america. *Conservation Biology*, 26(1):78–87.

Cayuela, H., Rougemont, Q., Prunier, J. G., Moore, J.-S., Clobert, J., Besnard, A., and Bernatchez, L. (2018). Demographic and genetic approaches to study dispersal in wild animal populations: A methodological review. *Molecular ecology*, 27(20):3976–4010.

Childress, W. M., Rykiel, E. J., Forsythe, W., Li, B.-L., and Wu, H.-i. (1996). Transition rule complexity in grid-based automata models. *Landscape Ecology*, 11(5):257–266.

Chubaty, A. M., Galpern, P., and Doctolero, S. C. (2020). The r toolbox grainscape for modelling and visualizing landscape connectivity using spatially explicit networks. *Methods in Ecology and Evolution*, 11(4):591–595.

Churko, G., Kienast, F., and Bolliger, J. (2020). A multispecies assessment to identify the functional connectivity of amphibians in a human-dominated landscape. *ISPRS International Journal of Geo-Information*, 9(5):287.

Clauzel, C. and Godet, C. (2020). Combining spatial modeling tools and biological data for improved multispecies assessment in restoration areas. *Biological Conservation*, 250:108713.

Compton, B., McGarigal, K., Cushman, S., and Gamble, L. (2007). A resistant kernel model of connectivity for vernal pool breeding amphibians. *Conserv Biol*, 21:788–799.

Confederation Suisse (2020). STAT-TAB-Interactive tables (FSO). Permanent and non permanent resident population by year, Canton, population type, residence permit, sex, age class and citizenship.

Crookston, N. L. and Dixon, G. E. (2005). The forest vegetation simulator: a review of its structure, content, and applications. *Computers and Electronics in Agriculture*, 49(1):60–80.

Csardi, G. and Nepusz, T. (2006). The igraph software package for complex network research. *InterJournal*, Complex Systems:1695.

Cushman, S. A., McRae, B., Adriaensen, F., Beier, P., Shirley, M., and Zeller, K. (2013). Biological corridors and connectivity [chapter 21]. *In: Macdonald, DW; Willis, KJ, eds. Key Topics in Conservation Biology 2. Hoboken, NJ: Wiley-Blackwell. p. 384-404.*, pages 384–404.

Dáttilo, W. and Rico-Gray, V. (2018). Ecological networks in the tropics. *Cham, Switzerland: Springer*.

Davis, M., Keighley, M., Naumann, S., and Graf, A. (2015). Green infrastructure and urban biodiversity: overview and city level examples. *ETC/BD report to the EEA*.

Di Cola, V., Broennimann, O., Petitpierre, B., Breiner, F. T., d'Amen, M., Randin, C., Engler, R., Pottier, J., Pio, D., Dubuis, A., et al. (2017). ecospat: an r package to support spatial analyses and modeling of species niches and distributions. *Ecography*, 40(6):774–787.

Diniz, M. F., Cushman, S. A., Machado, R. B., and De Marco Junior, P. (2020). Landscape connectivity modeling from the perspective of animal dispersal. *Landscape Ecology*, 35(1):41–58.

Donati, G. F., Bolliger, J., Psomas, A., Maurer, M., and Bach, P. M. (in press 2022). Reconciling cities with nature through blue-green infrastructure opportunities for regional biodiversity enhancement.

Duflot, R., Avon, C., Roche, P., and Bergès, L. (2018). Combining habitat suitability models and spatial graphs for more effective landscape conservation planning: An applied methodological framework and a species case study. *Journal for nature conservation*, 46:38–47.

Dunning, J. B., Danielson, B. J., and Pulliam, H. R. (1992). Ecological processes that affect populations in complex landscapes. *Oikos*, pages 169–175.

Elliot, N. B., Cushman, S. A., Macdonald, D. W., and Loveridge, A. J. (2014). The devil is in the dispersers: predictions of landscape connectivity change with demography. *Journal of Applied Ecology*, 51(5):1169–1178.

Estrada, E. and Bodin, Ö. (2008). Using network centrality measures to manage landscape connectivity. *Ecological Applications*, 18(7):1810–1825.

European Commission (2013). Communication from the Commission to the European Parliament, the Council, the European Economic and Social Commitee and the Commitee of the Regions. Green Infrastructure (GI) - Enhancing Europe's Natural Capital.

European Commission (2019). Guidance on a strategic framework for further supporting the deployment of EU-level green and blue infrastructure.

European Commission (2020). Communication from the Commission to the European Parliament, the Council, the European Economic and Social Commitee and the Commitee of the Regions. EU Biodiversity Strategy for 2030. bringing nature back into our lives.

Evans, J. S. (2021). *spatialEco*. R package version 1.3-6.

Fletcher Jr, R. J., Didham, R. K., Banks-Leite, C., Barlow, J., Ewers, R. M., Rosindell, J., Holt, R. D., Gonzalez, A., Pardini, R., Damschen, E. I., et al. (2018). Is habitat fragmentation good for biodiversity? *Biological conservation*, 226:9–15.

Freeman, L. C. (1977). A set of measures of centrality based on betweenness. *Sociometry*, pages 35–41.

Galpern, P., Manseau, M., and Fall, A. (2011). Patch-based graphs of landscape connectivity: a guide to construction, analysis and application for conservation. *Biological conservation*, 144(1):44–55.

Gironás, J., Roesner, L. A., Rossman, L. A., and Davis, J. (2010). A new applications manual for the storm water management model(swmm). *Environmental Modelling & Software*, 25(6):813–814.

Gower, J. C. (1971). A general coefficient of similarity and some of its properties. *Biometrics*, pages 857–871.

Grant, E. H. C., Muths, E., Schmidt, B. R., and Petrovan, S. O. (2019). Amphibian conservation in the anthropocene.

Grêt-Regamey, A., Sirén, E., Brunner, S. H., and Weibel, B. (2017). Review of decision support tools to operationalize the ecosystem services concept. *Ecosystem Services*, 26:306–315.

Guerry, A. D. and Hunter Jr, M. L. (2002). Amphibian distributions in a landscape of forests and agriculture: an examination of landscape composition and conf iguration. *Conservation Biology*, 16(3):745–754.

Hall, K. R., Anantharaman, R., Landau, V. A., Clark, M., Dickson, B. G., Jones, A., Platt, J., Edelman, A., and Shah, V. B. (2021). Circuitscape in julia: empowering dynamic approaches to connectivity assessment. *Land*, 10(3):301.

Hamel, P., Guerry, A., Polasky, S., Han, B., Douglass, J., Hamann, M., Janke, B., Kuiper, J., Levrel, H., Liu, H., et al. (2021). Mapping the benefits of nature in cities with the invest software. *Npj Urban Sustainability*, 1(1):1–9.

Hansen, S., Abrahamsen, P., Petersen, C., and Styczen, M. (2012). Daisy: Model use, calibration, and validation. *Transactions of the ASABE*, 55(4):1317–1333.

Holland, E. P., Aegerter, J. N., Dytham, C., and Smith, G. C. (2007). Landscape as a model: the importance of geometry. *PLoS Computational Biology*, 3(10):e200.

Horváth, Z., Ptacnik, R., Vad, C. F., and Chase, J. M. (2019). Habitat loss over six decades accelerates regional and local biodiversity loss via changing landscape connectance. *Ecology letters*, 22(6):1019–1027.

Jalali, Z. S., Rezvanian, A., and Meybodi, M. R. (2016). Social network sampling using spanning trees. *International Journal of Modern Physics C*, 27(05):1650052.

Kadoya, T. (2009). Assessing functional connectivity using empirical data. *Population ecology*, 51(1):5–15.

Karch (2022). Info fauna. centre de coordination pour la protection des amphibiens et reptiles de suisse (karch).

Keeley, A. T., Beier, P., and Gagnon, J. W. (2016). Estimating landscape resistance from habitat suitability: effects of data source and nonlinearities. *Landscape Ecology*, 31(9):2151–2162.

Keitt, T. H., Urban, D. L., and Milne, B. T. (1997). Detecting critical scales in fragmented landscapes. *Conservation ecology*, 1(1).

Kolaczyk, E. D. and Csárdi, G. (2014). *Statistical analysis of network data with R*, volume 65. Springer.

Kool, J. T., Moilanen, A., and Treml, E. A. (2013). Population connectivity: recent advances and new perspectives. *Landscape Ecology*, 28(2):165–185.

Kupfer, J. A. (2012). Landscape ecology and biogeography: rethinking landscape metrics in a post-fragstats landscape. *Progress in physical geography*, 36(3):400–420.

LaPoint, S., Balkenhol, N., Hale, J., Sadler, J., and van der Ree, R. (2015). Ecological connectivity research in urban areas. *Functional Ecology*, 29(7):868–878.

Lookingbill, T. R. and Minor, E. S. (2017). Assessing multi-scale landscape connectivity using network analysis. In *Learning Landscape Ecology*, pages 193–209. Springer.

Luke, D. A. (2015). *A user's guide to network analysis in R*, volume 72. Springer.

Luo, Y. and Wu, J. (2021). Linking the minimum spanning tree and edge betweenness to understand arterial corridors in an ecological network. *Landscape Ecology*, 36(5):1549–1565.

Maechler, M., Rousseeuw, P., Struyf, A., Hubert, M., and Hornik, K. (2021). *cluster: Cluster Analysis Basics and Extensions*. R package version 2.1.2 — For new features, see the 'Changelog' file (in the package source).

Manenti, R., Ficetola, G. F., and De Bernardi, F. (2009). Water, stream morphology and landscape: complex habitat determinants for the fire salamander salamandra salamandra. *Amphibia-Reptilia*, 30(1):7–15.

Matsler, A. M., Meerow, S., Mell, I. C., and Pavao-Zuckerman, M. A. (2021). A 'green'chameleon: Exploring the many disciplinary definitions, goals, and forms of "green infrastructure". *Landscape and Urban Planning*, 214:104145.

McNeil, B. E., Martell, R. E., and Read, J. M. (2006). Gis and biogeochemical models for examining the legacy of forest disturbance in the adirondack park, ny, usa. *Ecological Modelling*, 195(3-4):281–295.

McRae, B. H., Dickson, B. G., Keitt, T. H., and Shah, V. B. (2008a). Using circuit theory to model connectivity in ecology, evolution, and conservation. *Ecology*, 89(10):2712–2724.

McRae, B. H., Schumaker, N. H., McKane, R. B., Busing, R. T., Solomon, A. M., and Burdick, C. A. (2008b). A multi-model framework for simulating wildlife population response to land-use and climate change. *Ecological modelling*, 219(1-2):77–91.

Melián, C. J. and Bascompte, J. (2002). Complex networks: two ways to be robust? *Ecology Letters*, 5(6):705–708.

Minor, E. S. and Urban, D. L. (2008). A graph-theory framework for evaluating landscape connectivity and conservation planning. *Conservation biology*, 22(2):297–307.

Monteiro, R., Ferreira, J. C., and Antunes, P. (2020). Green infrastructure planning principles: An integrated literature review. *Land*, 9(12):525.

Murtagh, F. and Legendre, P. (2014). Ward's hierarchical agglomerative clustering method: which algorithms implement ward's criterion? *Journal of classification*, 31(3):274–295.

Newman, M. E. (2006). Modularity and community structure in networks. *Proceedings of the national academy of sciences*, 103(23):8577–8582.

Norton, B. A., Evans, K. L., and Warren, P. H. (2016). Urban biodiversity and landscape ecology: patterns, processes and planning. *Current Landscape Ecology Reports*, 1(4):178–192.

OpenStreetMap contributors (2022). Planet dump retrieved from https://planet.osm.org . `https://www.openstreetmap.org`.

Pascual-Hortal, L. and Saura, S. (2006). Comparison and development of new graph-based landscape connectivity indices: towards the priorization of habitat patches and corridors for conservation. *Landscape ecology*, 21(7):959–967.

Pearson, R. G., Raxworthy, C. J., Nakamura, M., and Townsend Peterson, A. (2007). Predicting species distributions from small numbers of occurrence records: a test case using cryptic geckos in madagascar. *Journal of biogeography*, 34(1):102–117.

Pebesma, E. (2018). Simple Features for R: Standardized Support for Spatial Vector Data. *The R Journal*, 10(1):439–446.

Pedersen, T. L. (2020). *tidygraph: A Tidy API for Graph Manipulation*. R package version 1.2.0.

Préau, C., Grandjean, F., Sellier, Y., Gailledrat, M., Bertrand, R., and Isselin-Nondedeu, F. (2020). Habitat patches for newts in the face of climate change: local scale assessment combining niche modelling and graph theory. *Scientific reports*, 10(1):1–13.

Prim, R. C. (1957). Shortest connection networks and some generalizations. *The Bell System Technical Journal*, 36(6):1389–1401.

PUB Singapore (2014). *Active Beautiful Clean Waters: Design Guidelines*. Public Utilities Board ("PUB"), Singapore.

Pyron, R. A. and Wiens, J. J. (2011). A large-scale phylogeny of amphibia including over 2800 species, and a revised classification of extant frogs, salamanders, and caecilians. *Molecular phylogenetics and evolution*, 61(2):543–583.

Ray, N. and Burgman, M. A. (2006). Subjective uncertainties in habitat suitability maps. *Ecological modelling*, 195(3-4):172–186.

Rossman, L. A. (1995). The epanet water quality model. Technical report, Environmental Protection Agency, Cincinnati, OH (United States).

Saura, S. and Pascual-Hortal, L. (2007). A new habitat availability index to integrate connectivity in landscape conservation planning: comparison with existing indices and application to a case study. *Landscape and urban planning*, 83(2-3):91–103.

Savard, J.-P. L., Clergeau, P., and Mennechez, G. (2000). Biodiversity concepts and urban ecosystems. *Landscape and urban planning*, 48(3-4):131–142.

Scheller, R. M., Domingo, J. B., Sturtevant, B. R., Williams, J. S., Rudy, A., Gustafson, E. J., and Mladenoff, D. J. (2007). Design, development, and application of landis-ii, a spatial landscape simulation model with flexible temporal and spatial resolution. *ecological modelling*, 201(3-4):409–419.

Schmidt, B. and Zumbach, S. (2005). Liste rouge des amphibiens menacés en Suisse. *Édit. Office fédéral de l'environnement, des forêts et du paysage (OFEFP), Berne, et Centre de coordination pour la protection des amphibiens et des reptiles de Suisse (KARCH), Berne. Série OFEFP: L'environnement pratique*, 46.

Shepard, D. (1968). A two-dimensional interpolation function for irregularly-spaced data. In *Proceedings of the 1968 23rd ACM national conference*, pages 517–524.

Singleton, P. H. (2002). *Landscape permeability for large carnivores in Washington: a geographic information system weighted-distance and least-cost corridor assessment*, volume 549. US Department of Agriculture, Forest Service, Pacific Northwest Research Station.

Stevenson-Holt, C. D., Watts, K., Bellamy, C. C., Nevin, O. T., and Ramsey, A. D. (2014). Defining landscape resistance values in least-cost connectivity models for the invasive grey squirrel: a comparison of approaches using expert-opinion and habitat suitability modelling. *PloS one*, 9(11):e112119.

Stöckle, C. O., Donatelli, M., and Nelson, R. (2003). Cropsyst, a cropping systems simulation model. *European journal of agronomy*, 18(3-4):289–307.

Taylor, P. D., Fahrig, L., Henein, K., and Merriam, G. (1993). Connectivity is a vital element of landscape structure. *Oikos*, pages 571–573.

Thuiller, W., Georges, D., Engler, R., and Breiner, F. (2016). Ensemble platform for species distribution modeling. *R Package Version*, pages 3–1.

Tischendorf, L. and Fahrig, L. (2000). On the usage and measurement of landscape connectivity. *Oikos*, 90(1):7–19.

Trochet, A., Moulherat, S., Calvez, O., Stevens, V. M., Clobert, J., and Schmeller, D. S. (2014). A database of life-history traits of European amphibians. *Biodiversity Data Journal*, (2).

Urban, D. and Keitt, T. (2001). Landscape connectivity: a graph-theoretic perspective. *Ecology*, 82(5):1205–1218.

Urban, D. L., Minor, E. S., Treml, E. A., and Schick, R. S. (2009). Graph models of habitat mosaics. *Ecology letters*, 12(3):260–273.

Van der Meer, L., Abad, L., Gilardi, A., and Lovelace, R. (2022). *sfnetworks: Tidy Geospatial Networks*. https://luukvdmeer.github.io/sfnetworks/

van der Sluis, T. and Jongman, R. (2021). Green infrastructure and network coherence. In *Handbook B: Scientific support for successful implementation of the Natura 2000 network*:, pages 24–78. European Commission.

Villéger, S., Mason, N. W., and Mouillot, D. (2008). New multidimensional functional diversity indices for a multifaceted framework in functional ecology. *Ecology*, 89(8):2290–2301.

Watts, D. J. and Strogatz, S. H. (1998). Collective dynamics of 'small-world'networks. *nature*, 393(6684):440–442.

Weichao, X., YUNHE, H., Hung, Y., and YUEXIAN, Z. (2010). Comparison of spearman's rho and kendall's tau in normal and contaminated normal models. *Manuscript submitted to IEEE Transactions on Information Theory (http://arxiv. org/PS_cache/arxiv/pdf/1011/1011.2009 v1. pdf)*.

Wickham, H., François, R., Henry, L., and Müller, K. (2021). *dplyr: A Grammar of Data Manipulation*. R package version 1.0.7.

Wiegand, T., Moloney, K. A., Naves, J., and Knauer, F. (1999). Finding the missing link between landscape structure and population dynamics: a spatially explicit perspective. *The american naturalist*, 154(6):605–627.

Wong, T. H., Fletcher, T. D., Duncan, H. P., Coleman, J. R., and Jenkins, G. A. (2002). A model for urban stormwater improvement: conceptualization. In *Global Solutions for Urban Drainage*, pages 1–14.

World Economic Forum (2022). Global risks report 2022, 17th edition.

Wu, J. (2014). Urban ecology and sustainability: The state-of-the-science and future directions. *Landscape and urban planning*, 125:209–221.

Zeller, K. A., McGarigal, K., and Whiteley, A. R. (2012). Estimating landscape resistance to movement: a review. *Landscape ecology*, 27(6):777–797.

Zhao, S.-m., Ma, Y.-f., Wang, J.-l., and You, X.-y. (2019). Landscape pattern analysis and ecological network planning of tianjin city. *Urban forestry & urban greening*, 46:126479.

List of Figures

List of Tables

Listings

Appendices

A Appendix: Visual comparison with Donati et al. (2022) 30 m resolution current maps

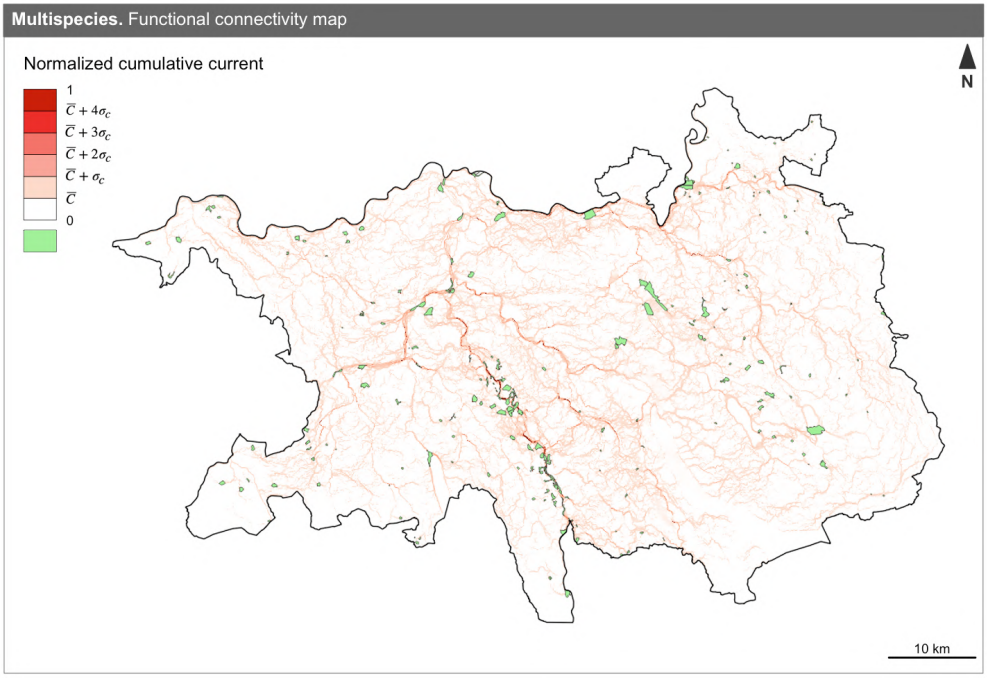

(a) Multi-species cumulative current. Donati et al. (2022) 30 m raster.

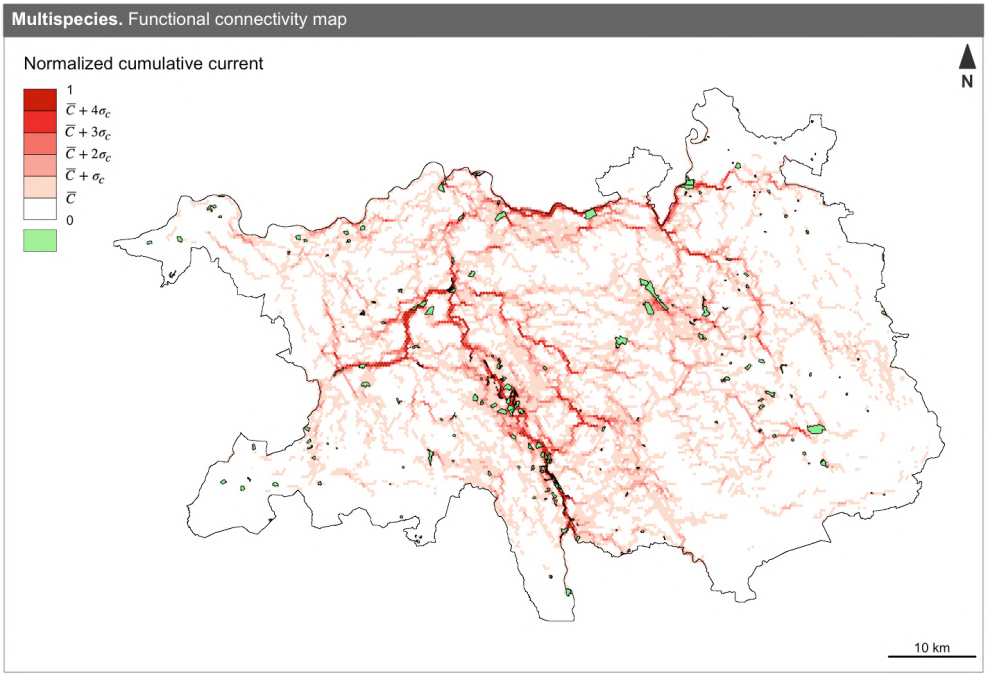

(b) Multi-species cumulative current. 300 m hexagonal grid.

Figure 4.1. Visual comparison with Donati et al. (2022) 30 m resolution current maps.

B Appendix: Simulation setups and computation times

Connectivity	Study area	Resolution	Representation	Nodes	Edges	Focal nodes	Species	Computation time
Functional	Cantons ZH - AG	100 m	Squared gri	316'427	629'886	4'579	*A. obstetricans*	Not feasible
							B. variegata	Not feasible
							H. arborea	Not feasible
							S. salamandra	Not feasible
			Hexagonal grid	316'122	943'488	4'712	*A. obstetricans*	Not feasible
							B. variegata	Not feasible
							H. arborea	Not feasible
							S. salamandra	Not feasible
		300 m	Squared grid	35'800	70'673	860	*A. obstetricans*	17h 18min
							B. variegata	19h 08min
							H. arborea	20h 56min
							S. salamandra	22h 46min
			Hexagonal grid	35'753	105'717	885	*A. obstetricans*	19h 59min
							B. variegata	22h 15min
							H. arborea	23h 37min
							S. salamandra	24h 16min
Structural	Top node 1	10 m	Raster format			126	*A. obstetricans*	55min
							B. variegata	57min
							H. arborea	58min
							S. salamandra	1h 07min
	Top node 2	10 m	Raster format			126	*A. obstetricans*	29min
							B. variegata	36min
							H. arborea	35min
							S. salamandra	50min
	Top node 3	10 m	Raster format			126	*A. obstetricans*	1h 01min
							B. variegata	50min
							H. arborea	1h 00min
							S. salamandra	1h 28min

Table 4.1. Simulation setups and computation times.

C Appendix: Single-species functional connectivity maps

C.1 Single-species current maps

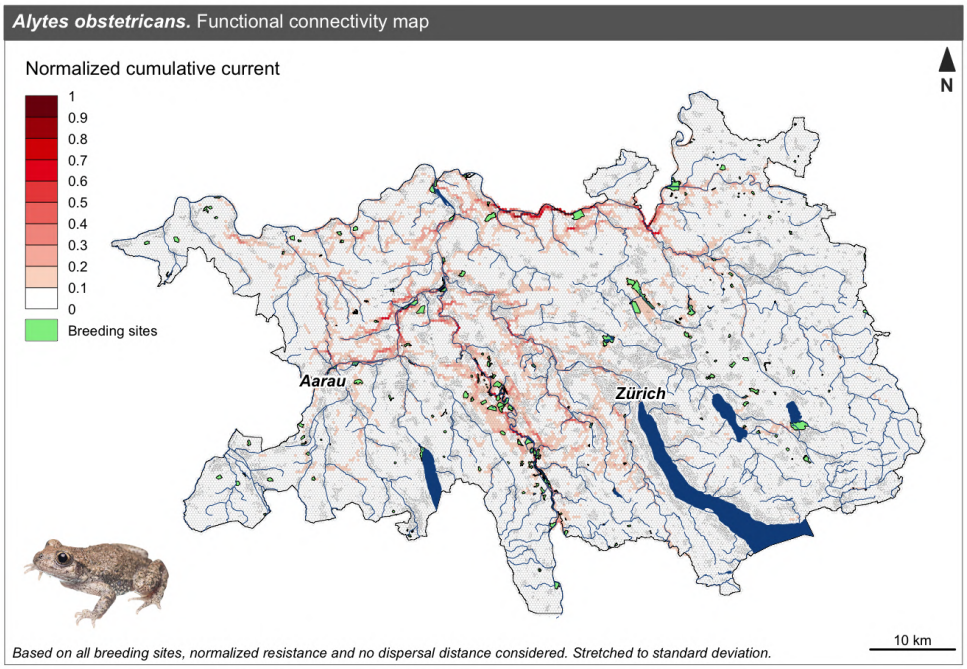

(a) Overview of the study area

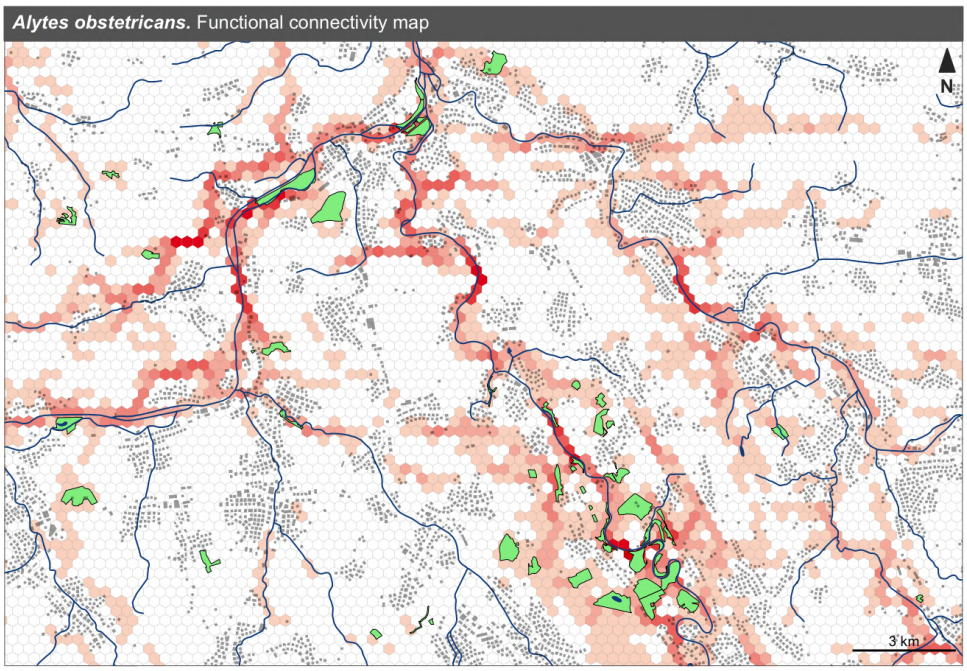

(b) Zoom in on the surroundings of Brugg

Figure 4.2. Alytes obstetricans normalized cumulative currents (hexagonal grid).

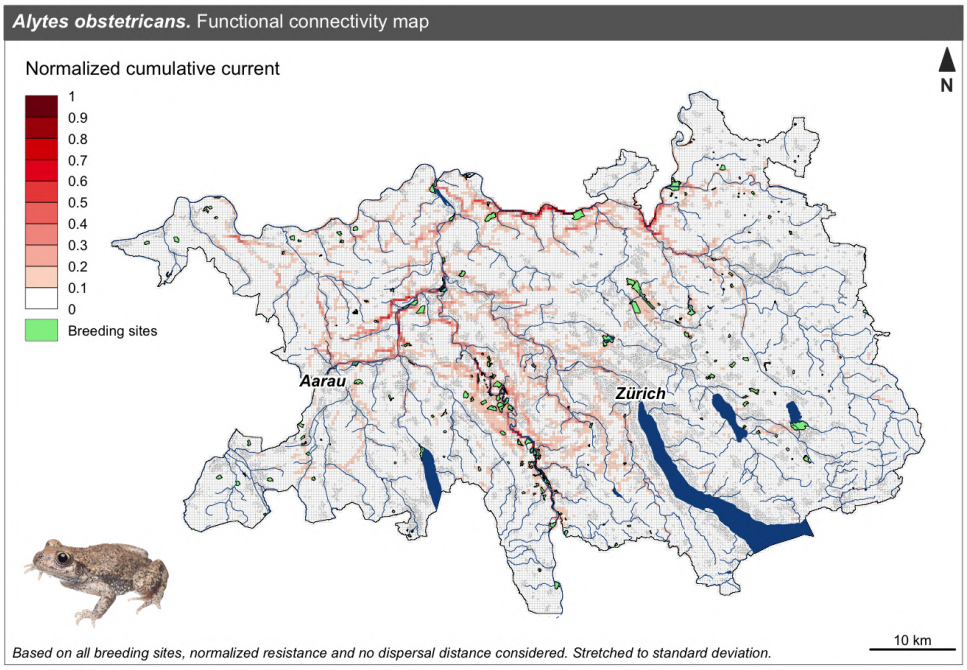

(a) Overview of the study area

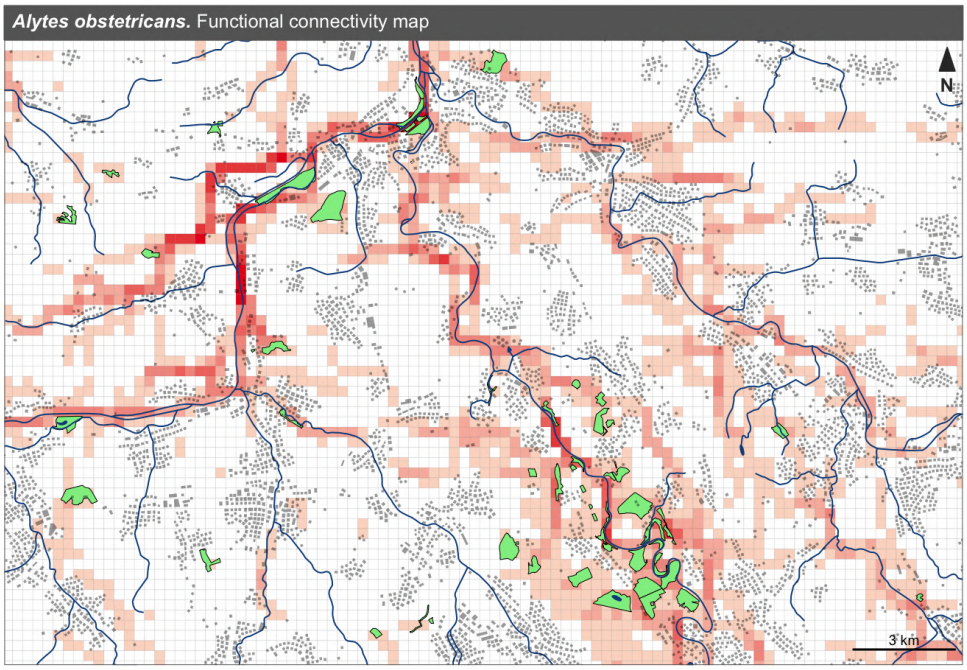

(b) Zoom in on the surroundings of Brugg

Figure 4.3. Alytes obstetricans normalized cumulative currents (squared grid).

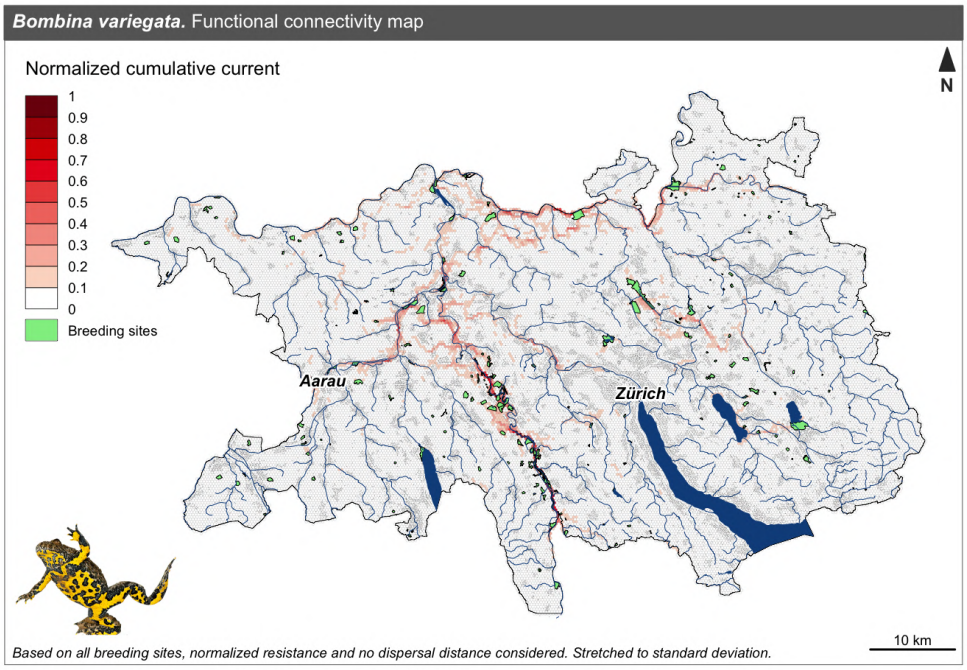

(a) Overview of the study area

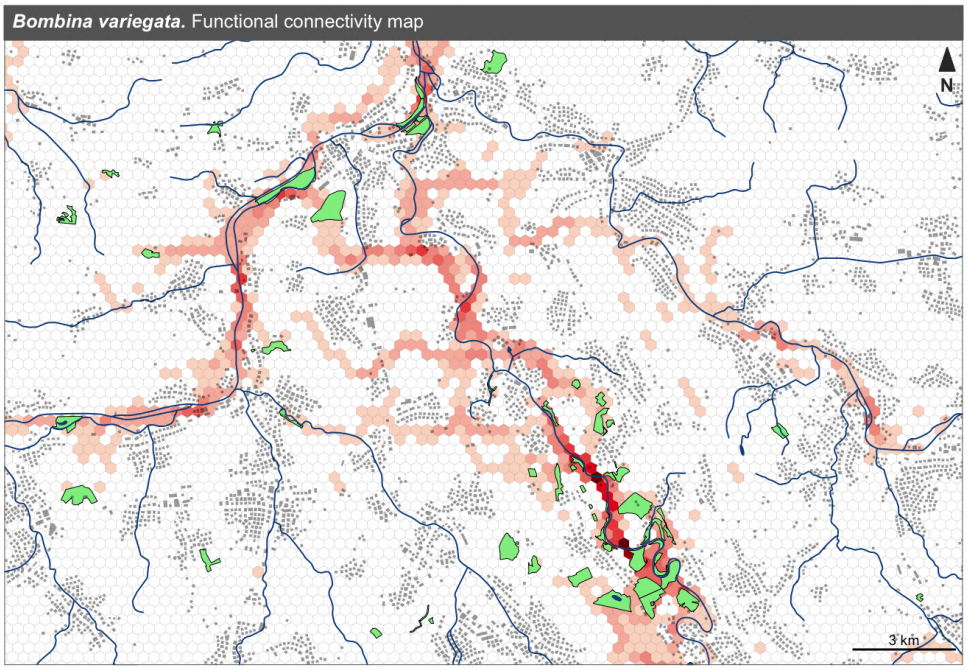

(b) Zoom in on the surroundings of Brugg

Figure 4.4. Bombina variegata normalized cumulative currents (hexagonal grid).

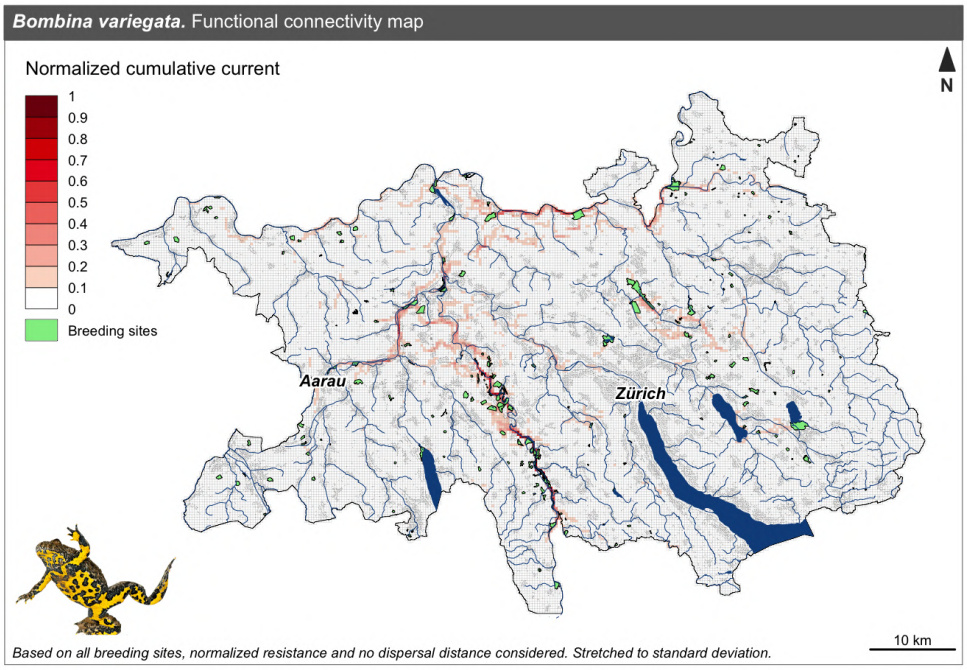

(a) Overview of the study area

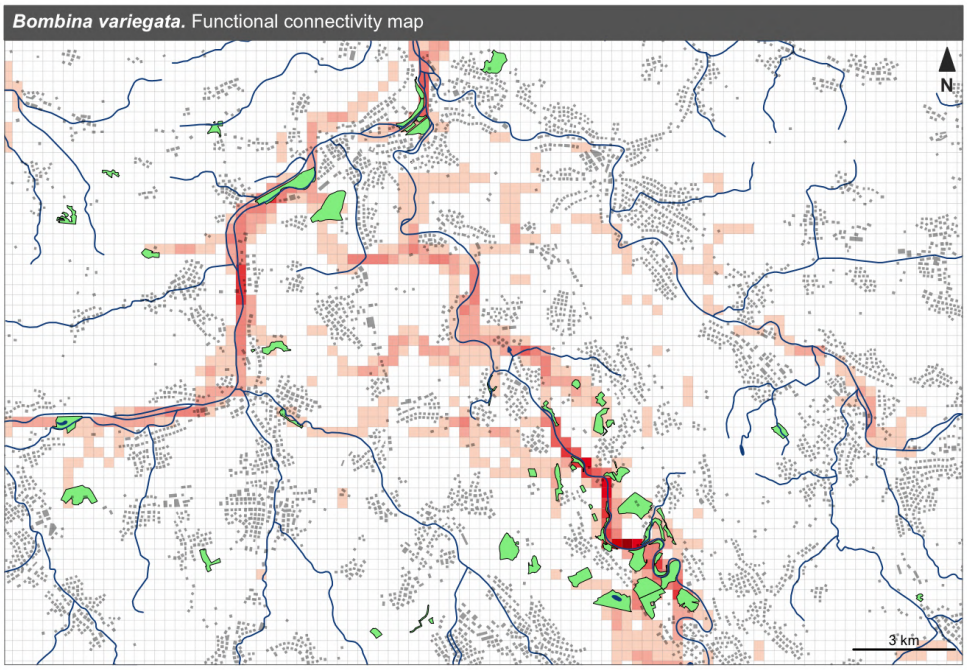

(b) Zoom in on the surroundings of Brugg

Figure 4.5. Bombina variegata normalized cumulative currents (squared grid).

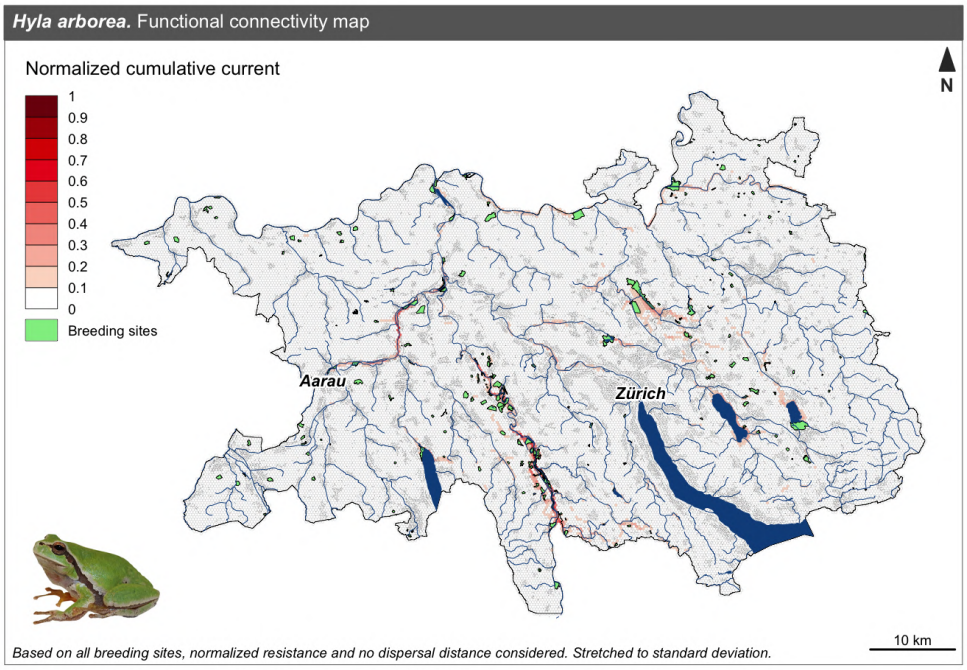

(a) Overview of the study area

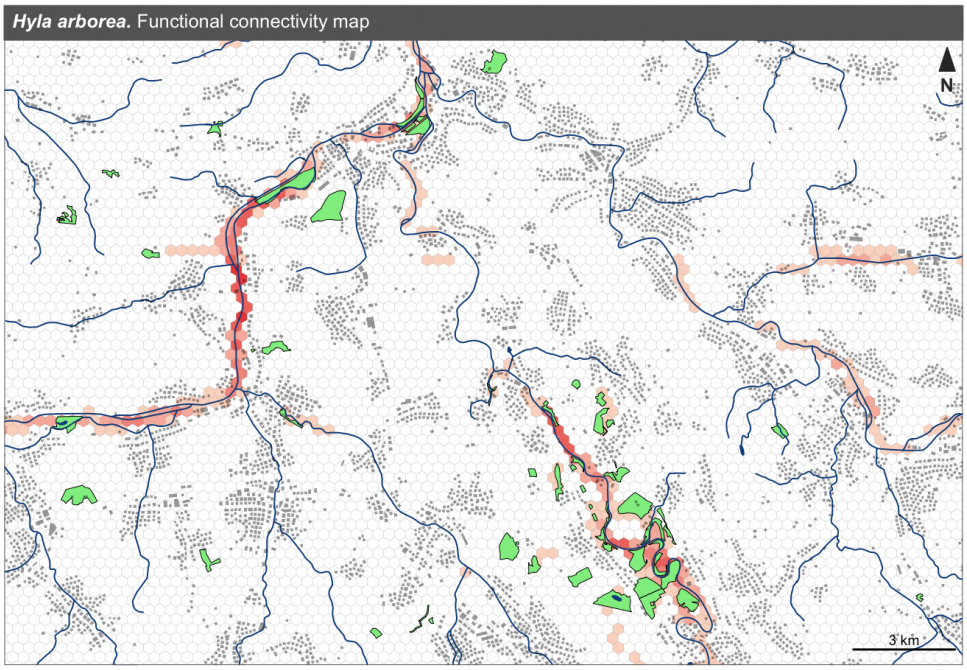

(b) Zoom in on the surroundings of Brugg

Figure 4.6. Hyla arborea normalized cumulative currents (hexagonal grid).

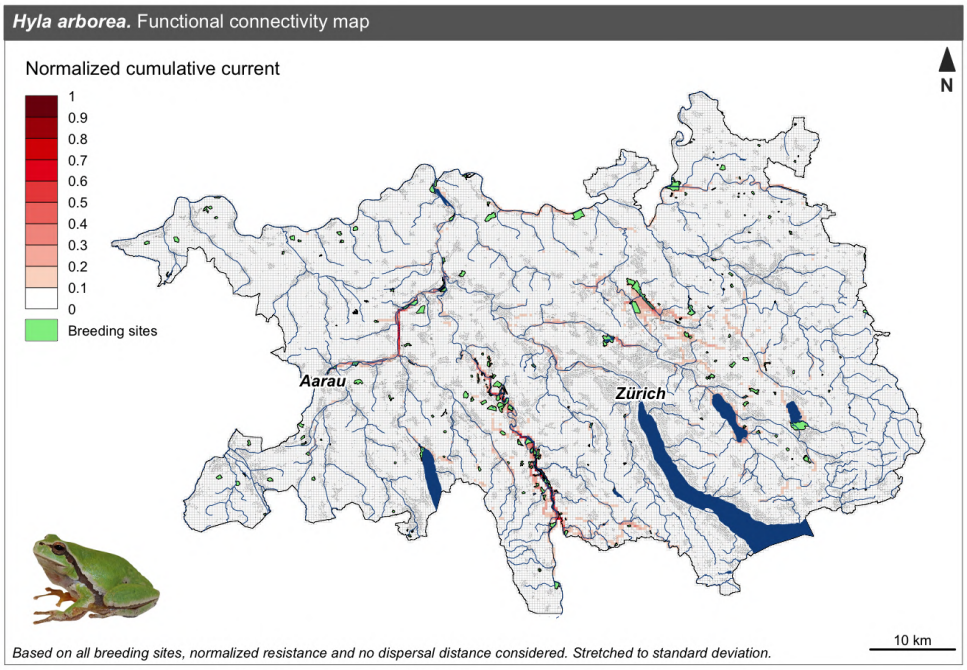

(a) Overview of the study area

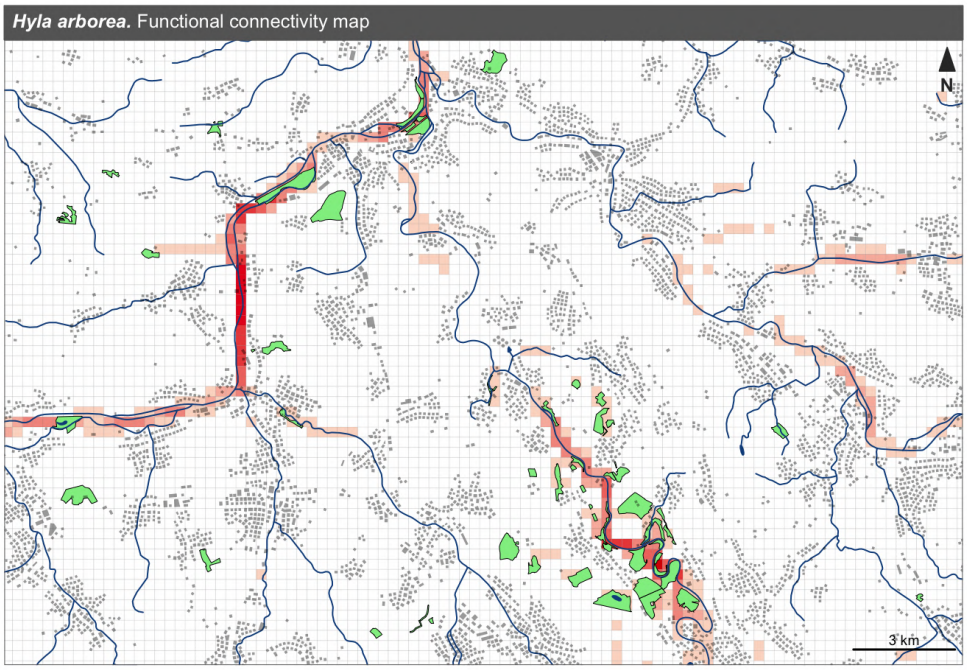

(b) Zoom in on the surroundings of Brugg

Figure 4.7. Hyla arborea normalized cumulative currents (squared grid).

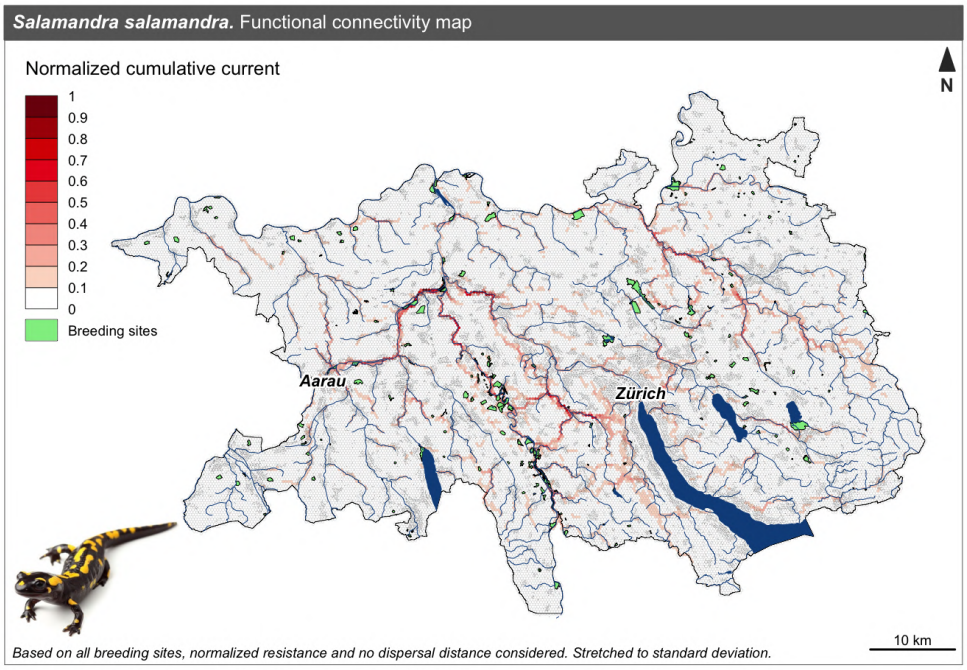

(a) Overview of the study area

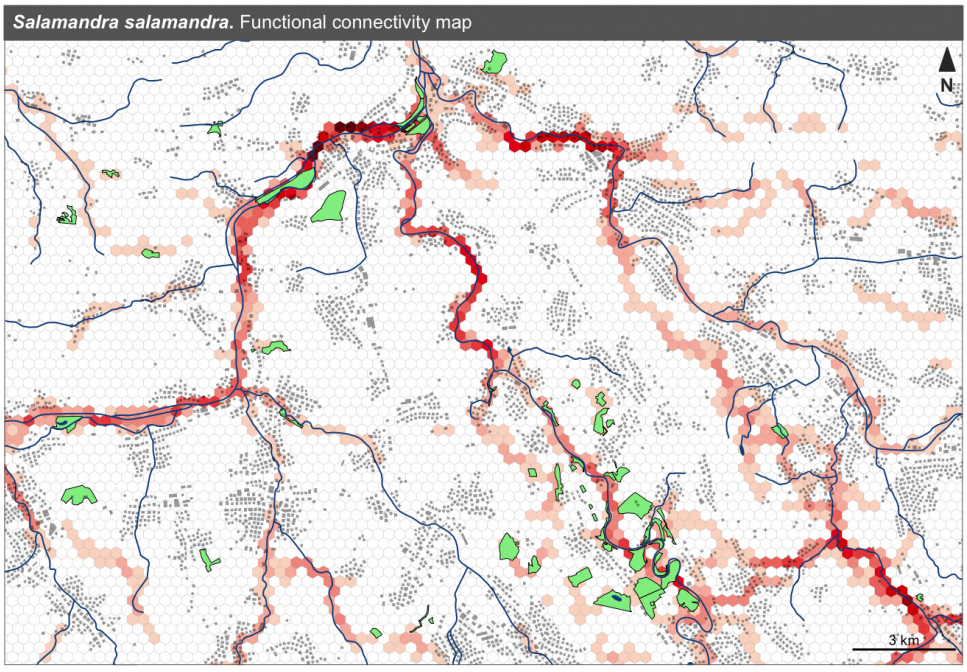

(b) Zoom in on the surroundings of Brugg

Figure 4.8. Salamandra salamandra normalized cumulative currents (hexagonal grid).

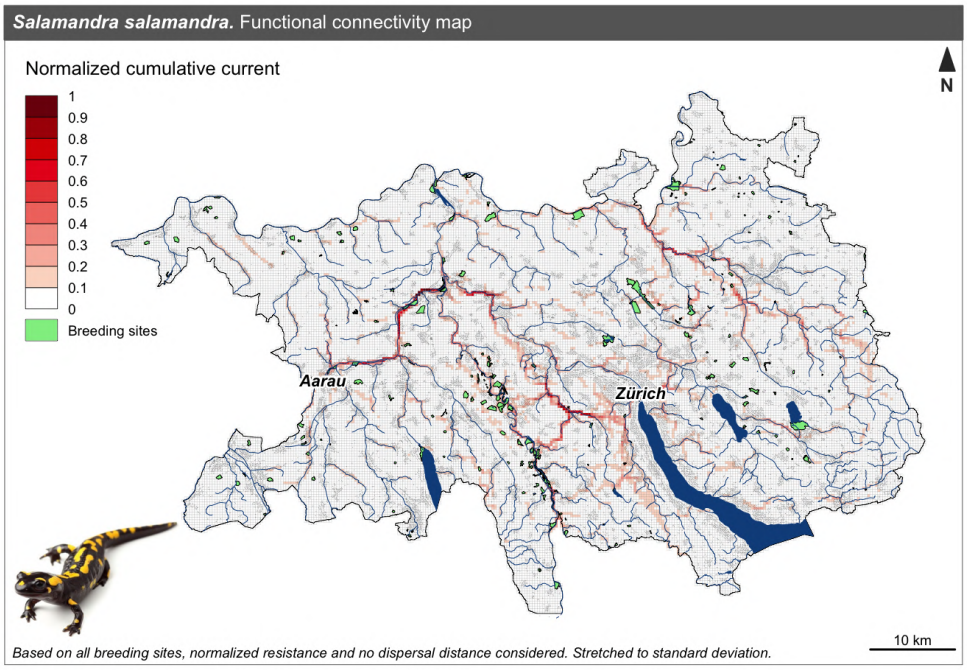

(a) Overview of the study area

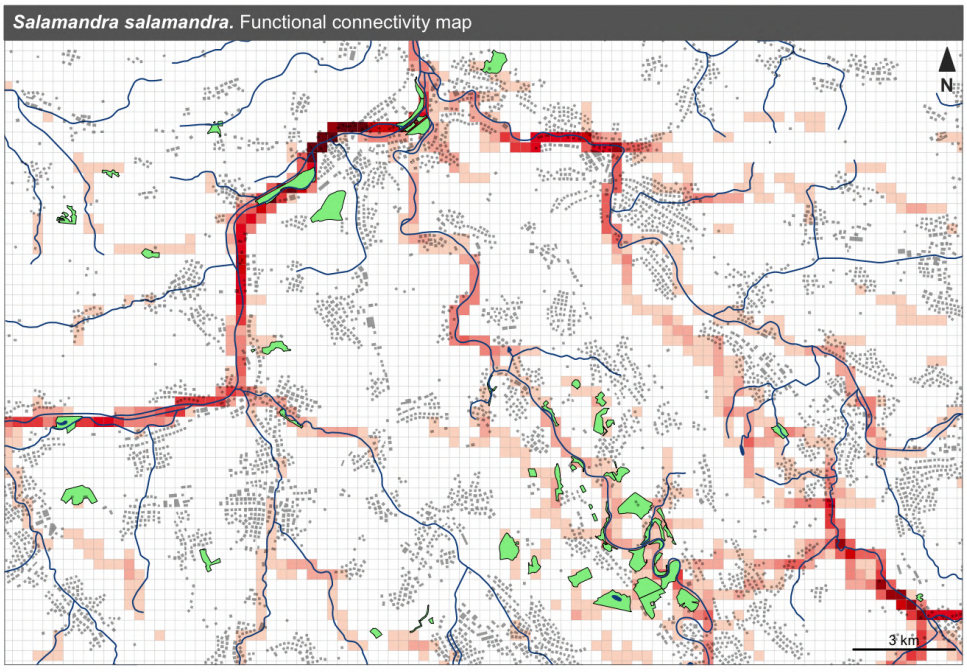

(b) Zoom in on the surroundings of Brugg

Figure 4.9. Salamandra salamandra normalized cumulative currents (squared grid).

C.2 Multi-species current maps

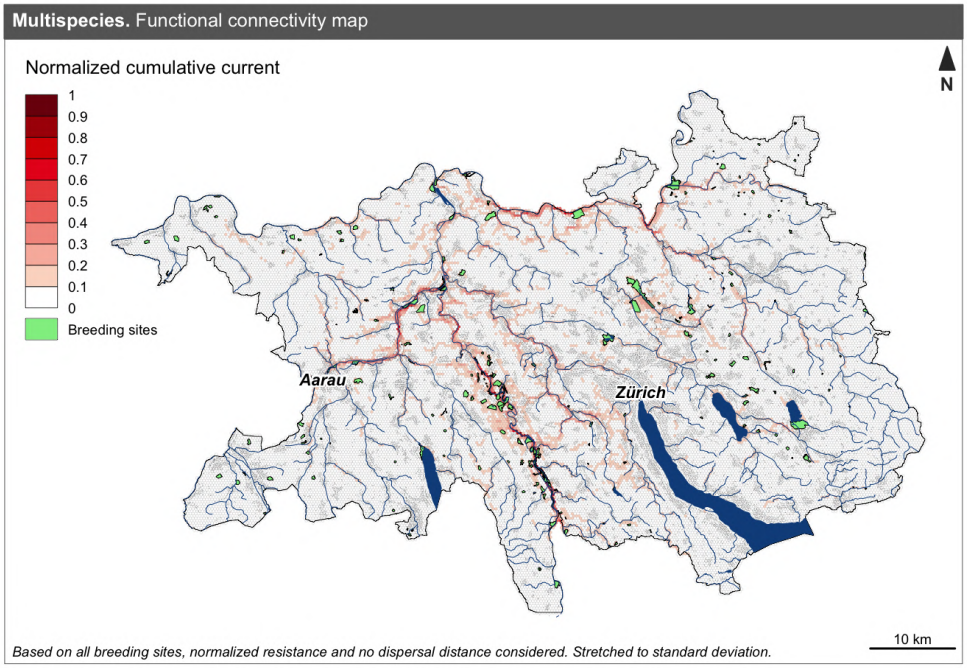

(a) Overview of the study area

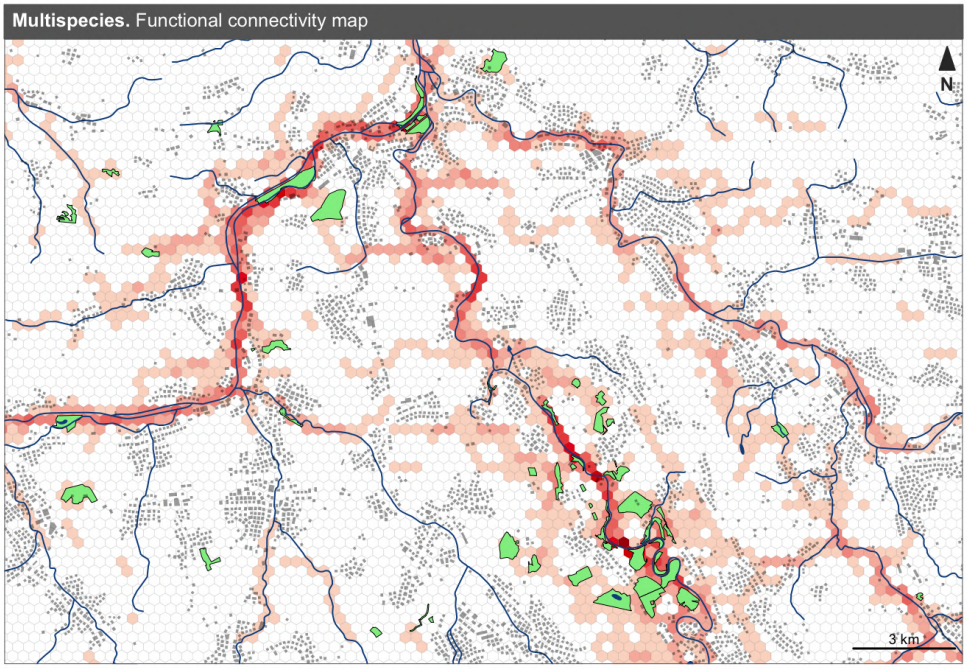

(b) Zoom in on the surroundings of Brugg

Figure 4.10. Multi-species normalized cumulative current (hexagonal grid).

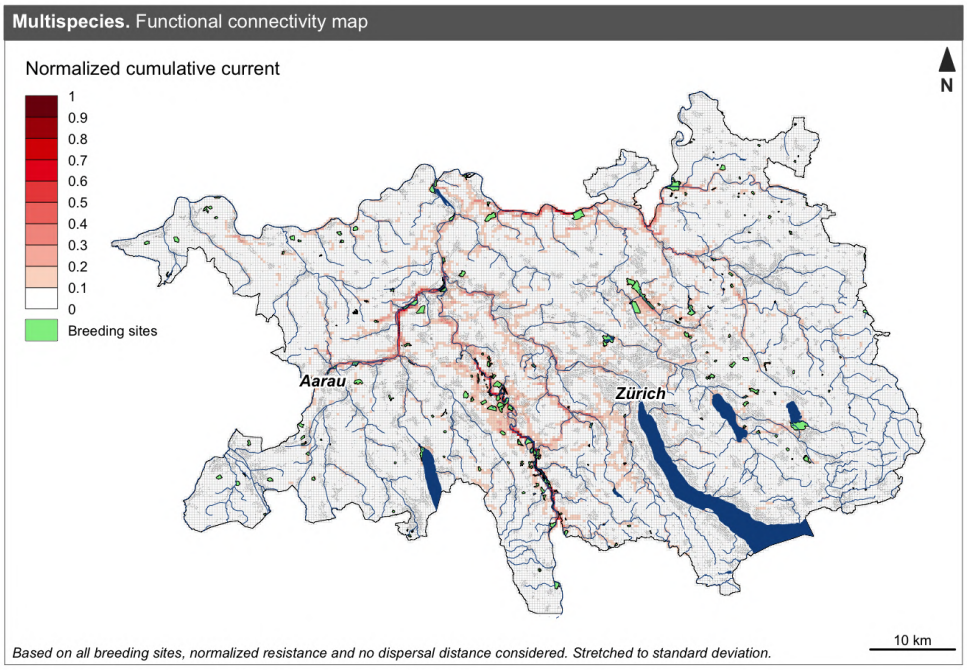

(a) Overview of the study area

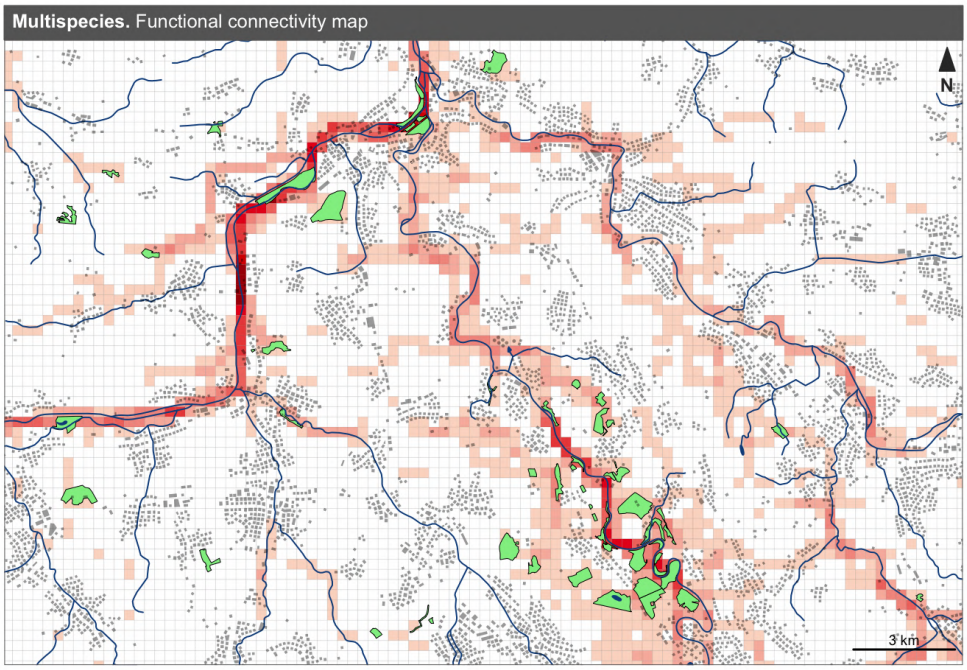

(b) Zoom in on the surroundings of Brugg

Figure 4.11. Multi-species normalized cumulative current (squared grid).

D Appendix: Edge thresholding experiments

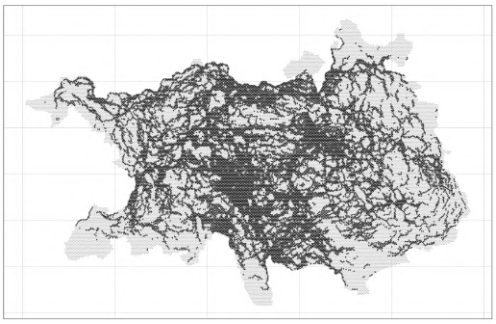

(a) $C \geq \overline{C}$

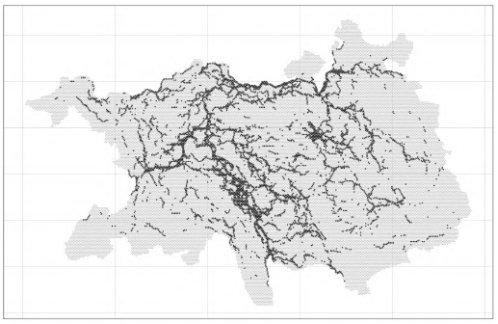

(b) $C \geq \overline{C} + \sigma_c$

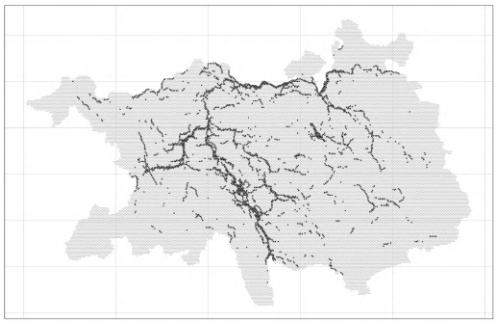

(c) $C \geq \overline{C} + 2\sigma_c$

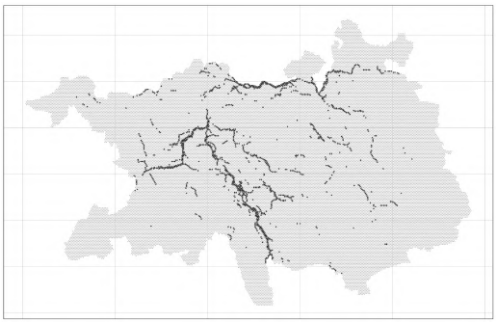

(d) $C \geq \overline{C} + 3\sigma_c$

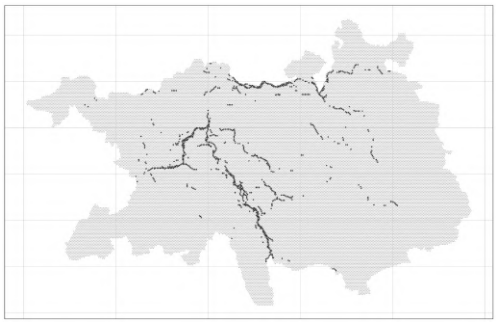

(e) $C \geq \overline{C} + 4\sigma_c$

Figure 4.12. Edge thresholding experiments.

E Appendix: Environmental variables at Top node 1

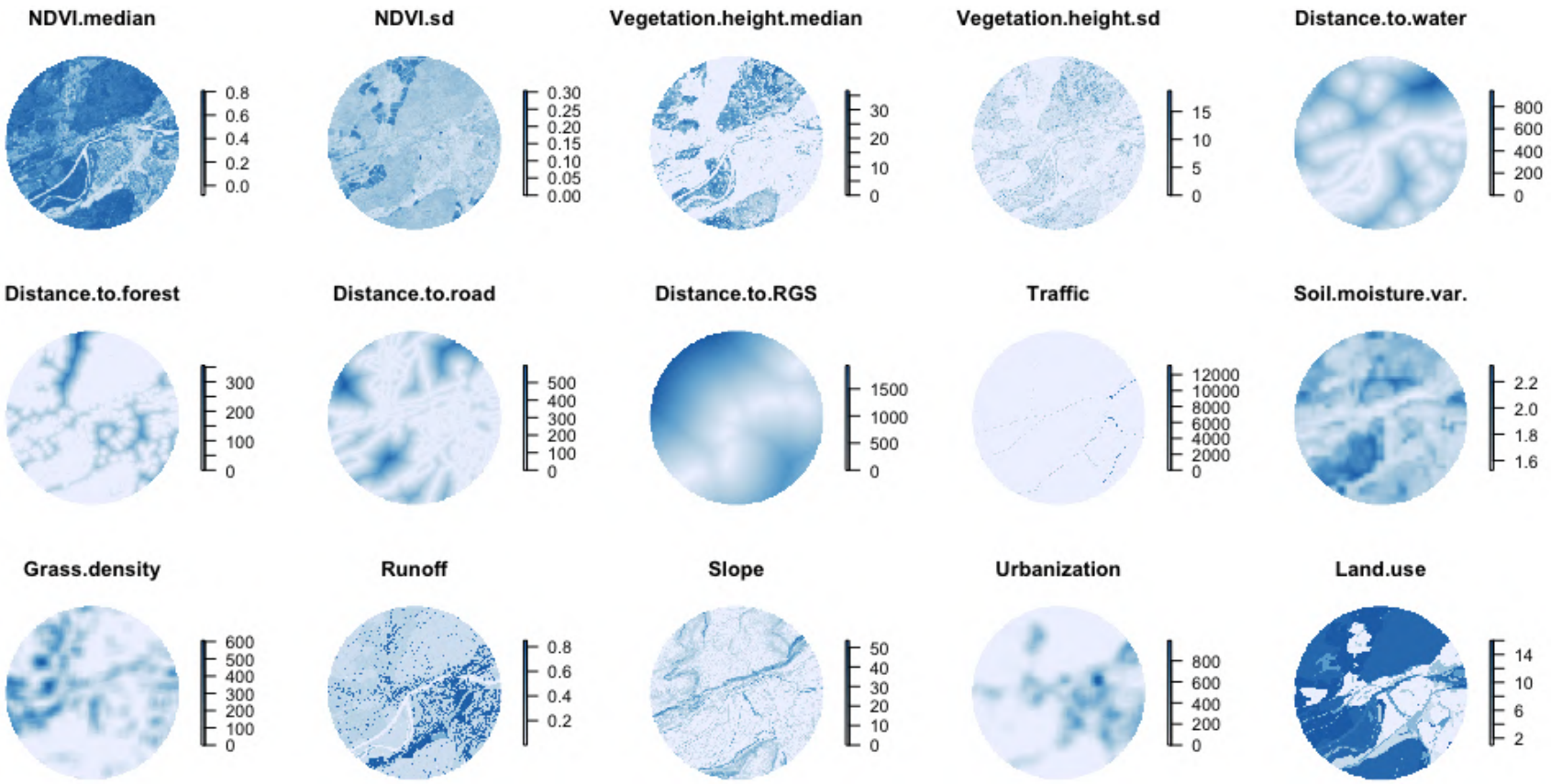

Figure 4.13. Environmental variables at the top node 1.